Published for SISSA by Springer

Received: *May 28, 2026*
Accepted: *August 26, 2026*
Published: *October 5, 2026*

Exclusive dimuon production and coherent charmonium photoproduction at forward rapidity in ultra-peripheral Pb–Pb collisions at $\sqrt{s_{\rm NN}} = 5.36$ TeV



The ALICE collaboration

Full author list at the end of the paper

E-mail: alice-publications@cern.ch

Abstract: This Paper presents rapidity-differential measurements of coherent J/ψ and ψ(2S) photoproduction, as well as rapidity- and mass-differential measurements of exclusive dimuon production, in the forward rapidity region $-4 < y < -2.5$ in ultra-peripheral Pb–Pb collisions at $\sqrt{s_{\rm NN}} = 5.36$ TeV using data recorded by the ALICE detector at the LHC in 2023, corresponding to an integrated luminosity of $\mathcal{L} = 1170 \pm 50\,\mu\text{b}^{-1}$. The J/$\psi$ and ψ(2S) results reveal the significant role of nuclear shadowing effects. The square root of the ratio of the measured quarkonium cross section to the impulse approximation prediction is about 0.76 for J/ψ and 0.71 for ψ(2S), at $y \approx -3$, corresponding to typical Bjorken-x values of 10^{-2}. The exclusive dimuon results highlight the sensitivity of such measurements to precise modeling of the photon flux, particularly at impact parameters near the nuclear radius.

Keywords: Heavy Ion Experiments, Photon Production, Quarkonium

ArXiv ePrint: 2605.13569

Open Access, Copyright CERN,
for the benefit of the ALICE Collaboration.
Article funded by SCOAP^3.

https://doi.org/10.1007/JHEP10(2026)057

JHEP10(2026)057

Contents

1 Introduction **1**

2 Experimental setup **3**

3 Data analysis **4**
3.1 Systematic uncertainties 8

4 Results and discussion **11**
4.1 Coherent J/ψ and ψ(2S) cross sections 11
4.2 Cross section of exclusive dimuon production 13

5 Conclusion **14**

The ALICE collaboration **24**

1 Introduction

Ultra-peripheral heavy-ion collisions (UPC) occur when two heavy ions pass by each other at impact parameters greater than the sum of the radii of the incoming nuclei [1]. These events are characterized by the dominant role of strong electromagnetic fields generated by the charged nuclei, which can be described using the equivalent photon approximation (EPA) and treated as fluxes of quasi-real photons with small virtuality, $q^2 < (\hbar c/R_A)^2$, where R_A is the nuclear radius. The distinctive properties of UPCs provide a unique opportunity to study photon-photon and photonuclear interactions in a clean environment, in particular through vector meson photoproduction and exclusive dimuon production.

Vector mesons (such as J/ψ, ψ(2S)) can be produced in a photonuclear interaction either coherently or incoherently. In the former case, the incoming photon interacts with the entire nucleus, while in the latter case, it interacts with a single nucleon inside the nucleus. Coherent interaction (figure 1, left) results in a lower transverse momentum (p_{T}) of the produced vector meson, with $\langle p_{\mathrm{T}} \rangle \sim 50$ MeV/c, while incoherent interaction leads to a higher transverse momentum with $\langle p_{\mathrm{T}} \rangle \sim 500$ MeV/c. Incoherent production is often accompanied by nuclear breakup with fragments and nucleons going in the very forward direction. In addition, an incoherent process can lead to the excitation and dissociation of the target nucleon, resulting in vector meson production at transverse momenta of $p_{\mathrm{T}} \sim 1$ GeV/c and above [2].

In the leading-logarithmic approximation of perturbative QCD (pQCD), the coherent J/ψ and ψ(2S) photoproduction is sensitive to the gluon density in nuclei [3, 4], making these measurements valuable probes of nuclear shadowing and gluon saturation at low Bjorken-x. Beyond leading order, additional contributions complicate the direct interpretation of the cross sections solely in terms of the nuclear gluon density [5–7]. At the Large Hadron Collider (LHC) at CERN, charmonium photoproduction measurements probe a broad Bjorken-x range, $10^{-5} \lesssim x \lesssim 10^{-2}$, where $x = (m/\sqrt{s_{\mathrm{NN}}})e^{\pm y}$ for a vector meson of mass m and rapidity y produced in UPCs at the nucleon–nucleon center-of-mass energy $\sqrt{s_{\mathrm{NN}}}$. These measurements

JHEP10(2026)057

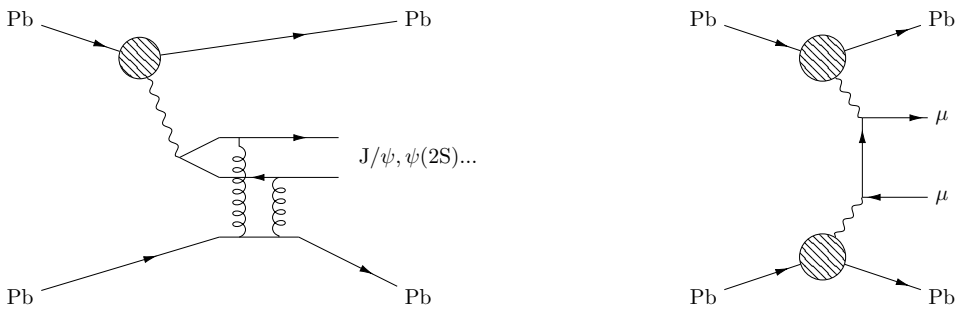


Figure 1. Leading-order diagrams for the coherent vector meson photoproduction (left) and for the exclusive dimuon production by photon fusion (right).

JHEP10(2026)057

therefore provide important constraints on nuclear partonic structure and enable tests of QCD-based descriptions of low-x dynamics, including the shadowing and saturation models compared with the present data [8–12].

Photoproduction of J/ψ off protons has been extensively studied at HERA in electron-proton collisions [13]. At the LHC, numerous results have been obtained for exclusive production of J/ψ and ψ(2S) in pp, p–Pb, and Pb–Pb collisions at different energies by ALICE [14–23], LHCb [24–28], CMS [29] and ATLAS [30]. At the Relativistic Heavy Ion Collider (RHIC) at BNL, measurements of exclusive J/ψ and ψ(2S) production were performed with Au–Au UPCs at $\sqrt{s_{\rm NN}}$ = 200 GeV by the STAR [31, 32] and PHENIX [33] collaborations. The exclusive J/ψ photoproduction cross section off protons measured in pp and p–Pb collisions exhibits a power-law growth with energy, showing no clear evidence of gluon saturation effects. At the same time, the suppression of coherent J/ψ photoproduction cross sections measured with respect to the impulse approximation in Pb–Pb UPCs can be well described by either calculations with nuclear parton distribution functions (nPDFs) or saturation-based models over a wide range of Bjorken-x values, from $\sim 10^{-5}$ to $\sim 10^{-3}$. Precise measurements of heavy vector meson production cross sections can provide crucial constraints on theoretical models aiming to explain the observed suppression.

The production of lepton pairs is a pure QED process that proceeds via photon-photon fusion (figure 1, right). The lepton-pair production cross section can be obtained by convoluting the two-photon luminosity with the leading-order elementary cross section of the Breit-Wheeler process [34]. Higher-order corrections commonly discussed in the context of dilepton production are related to the final-state radiation [35, 36], Coulomb and unitarity corrections [37, 38], the latter being still a subject of theoretical debate. The two-photon luminosity can be calculated within EPA by convoluting photon fluxes emitted by the nuclei. In a widely used Monte Carlo event generator STARlight [39, 40], photon fluxes are modeled using a well-known expression for a point-like source [41]. A hard cutoff at the nuclear radius is then applied, thus neglecting the flux of photons emitted at impact parameters smaller than the nuclear radius. In a more refined approach implemented in event generators such as SuperChic 4 [42, 43] and Upcgen [44, 45], photon fluxes are described using nuclear form factors accounting for photon impact parameters smaller than the nuclear radius, thereby allowing the possible production of lepton pairs inside nuclei.

Dilepton production measurements have been performed by ALICE in Pb–Pb [46] and p–Pb [20] UPCs, by CMS [47] and ATLAS [48, 49] in Pb–Pb UPCs, and by PHENIX [33] and STAR [31, 50, 51] in Au–Au UPCs, with the results being generally consistent with leading-order QED calculations. However, recent ATLAS results [48, 49] on dimuon and dielectron production in Pb–Pb UPCs show a discrepancy with STARlight calculations of up to 15–20% at large rapidities. It has been argued that accounting for photon-nucleus impact parameters smaller than the nuclear radius may help to resolve the discrepancy [38, 44, 52]. In addition, inclusion of higher-order QED contributions could improve the consistency between the data and theoretical predictions [38, 53].

In this Paper, we present results on coherent charmonium photoproduction and exclusive dimuon production measurements at forward rapidity $-4 < y < -2.5$ in Pb–Pb UPCs at a center-of-mass energy of $\sqrt{s_{\rm NN}} = 5.36$ TeV collected in 2023 with the upgraded ALICE detector.

2 Experimental setup

The ALICE detector [54] at the LHC was designed and constructed with the ability to cope with the high-multiplicity environment created in collisions of heavy ions. During the LHC Long Shutdown 2 (2019–2022), the ALICE detector underwent a significant revision, enabling the full potential of the LHC. The upgrade includes updated subsystems, enhanced readout electronics, a new Central Trigger Processor, and an upgraded data acquisition system. A detailed description of the upgrades can be found in ref. [55]. In the following, only the detector subsystems relevant for this analysis are described.

During the LHC Run 2 (2015–2018), the system of forward detectors comprising the V0 and T0 subsystems [56] served, among other purposes, as an interaction trigger and a luminometer, and was used to select UPCs by applying a veto on the activity associated with hadronic collisions. After the major Long Shutdown 2 upgrades, the new Fast Interaction Trigger (FIT) [57, 58] has replaced the aforementioned trigger system to provide an improved performance for the high interaction rates anticipated during the LHC Run 3 (2022–2026). The FIT system includes the FV0 and FT0 detectors used for vetoing of hadronic interactions and for luminosity measurements, respectively. The FV0 detector is composed of scintillator arrays, located at $z = 3.2$ m from the interaction point on the A-side of the ALICE experiment, covering the pseudorapidity range $2.2 < \eta < 5.1$. The FT0 consists of two arrays of quartz Cherenkov radiators installed on both sides of the interaction point and covering the pseudorapidity ranges $3.5 < \eta < 4.9$ and $-3.3 < \eta < -2.1$.

The ALICE experiment is equipped with two zero-degree calorimeters (ZDC) sensitive to the neutron emission, ZNA and ZNC [59, 60]. Located at ± 112.5 m from the interaction point along the beam direction, they are used to detect neutral particles produced at $|\eta| > 8.8$, and also serve as luminometers for heavy-ion collisions. The calorimeters are made of a tungsten alloy with embedded quartz fibers, with a total depth of 8.7 interaction lengths. The readout system was significantly upgraded in Run 3 to sustain interaction rates of 50 kHz and higher, without dead time in continuous readout mode. The operating conditions are exceptionally challenging considering that the ZDC not only covers nucleon emission from

JHEP10(2026)057

hadronic interactions but also those resulting from electromagnetic dissociation, which have ∼50 times higher cross sections in Pb–Pb collisions at LHC energies [61–65].

For the ALICE muon spectrometer, located on the C-side of the experiment at negative z with respect to the nominal interaction point, significant improvements were implemented in the readout electronics [58] of the Muon Tracking Chambers (MCH) and the Muon Identifier (MID) [54]. However, the overall detector implementation has remained unchanged. The muon spectrometer provides track reconstruction and muon identification capabilities in the forward rapidity region $-4 < \eta < -2.5$. It consists of a ten interaction-length absorber followed by the five tracking stations of the MCH detector, each containing two planes of cathode pad chambers. The third station is placed inside a dipole magnet with a 3 T·m integrated magnetic field. Downstream of the tracking stations, a 7.2 interaction-length iron wall is positioned to further reduce the remaining hadronic contamination, mainly from pion and kaon decay products. It is followed by the MID detector, constructed with four planes of resistive plate chambers.

The significant system upgrades implemented for the ALICE detector enabled the transition to the continuous readout mode and to process collisions at high interaction rates up to 1 MHz in pp and 50 kHz in Pb–Pb collisions. With the increased data sample, the precision of the coherent J/ψ cross section measurement can be improved in comparison to previous ALICE measurements at forward rapidity in Pb–Pb UPCs at $\sqrt{s_{\rm NN}} = 5.02$ TeV [16], enabling as well the first rapidity-differential measurement of the coherent ψ(2S) cross section. In addition, the absence of a hardware trigger on single-muon transverse momentum in the new continuous readout mode gives improved access to the exclusive dimuon production process, $\gamma\gamma \to \mu\mu$, at low invariant masses of muon pairs down to $m_{\mu\mu} \sim 1.5$ GeV/c^2. However, the new data-taking regime requires a careful reconsideration of the event selection strategy applied for UPCs in the forward rapidity region.

3 Data analysis

The study of coherent J/ψ and ψ(2S) photoproduction, and the exclusive dimuon production is based on a Pb–Pb data sample collected in 2023, corresponding to an integrated luminosity of $\mathcal{L} = 1170 \pm 50\ \mu\text{b}^{-1}$.

The integrated luminosity is estimated using reference triggers from the FT0 detector and the zero-degree calorimeters. The FT0 trigger selects events based on a signal amplitude threshold corresponding to the 50% centrality class, where centrality is defined as the percentile of hadronic Pb–Pb collisions, and determined from a Glauber model fit [66–68]. The cross sections for these reference triggers are extrapolated from the inelastic hadronic Pb–Pb cross section measured at $\sqrt{s_{\rm NN}} = 5.02$ TeV [63] to $\sqrt{s_{\rm NN}} = 5.36$ TeV using the Glauber model. The ZDC triggers, used for systematic uncertainty evaluation, require the detection of neutrons on at least one side of the experiment, making them sensitive to electromagnetic dissociation and hadronic interactions of colliding nuclei.

This analysis utilizes the muon spectrometer for track reconstruction and muon identification in the forward rapidity region. The event selection strategy requires a pair of muon tracks within the spectrometer acceptance and the absence of hadronic activity in the FV0 detector. Muon tracks are reconstructed in MCH using the tracking algorithm described in

JHEP10(2026)057

refs. [69, 70]. In the continuous readout mode, information from the detectors is acquired in samples corresponding to specific time intervals. The MCH readout frame (ROF) of 1 μs does not allow one to determine the timing of reconstructed MCH tracks with the required precision to resolve individual bunch crossing (BC) intervals, being about 25 ns. However, the precise timing provided by the MID detector can be used to determine the exact BC for MCH tracks matched to MID track segments (MCH-MID tracks). The MCH tracks are extrapolated to the MID detector surfaces, and the best-matching MID track segment is then selected by minimizing a χ^2 function constructed from the residuals between the MCH-track and MID-segment parameters.

This analysis relies on track timing information to construct candidates, as the primary vertex position is not reconstructed for UPCs. Candidate events are formed from pairs of oppositely charged MCH-MID tracks originating from the same BC. For the studies of the MCH-MID matching uncertainty, a less strict requirement is considered: if exactly one MCH-MID track is found in a given BC, an event candidate is constructed by attaching another MCH track in a sufficiently large $\pm$10 BC interval, covering most of the candidates.

In the constructed event candidates, each track is required to have a pseudorapidity within the muon spectrometer acceptance and a transverse momentum above 0.5 GeV/c. In order to ensure good track quality and to reduce background contamination originating from the beam-gas interactions, the tracks are required to pass additional selection criteria. Limits on the track radial coordinate at the absorber end are imposed $17.6 < R_{\rm abs} < 89.5$ cm in order to avoid regions of high multiple scattering. Furthermore, tracks must satisfy a selection criterion based on $p \times$ DCA, which is the product of the track momentum p and its distance of closest approach (DCA) to the nominal vertex at $z = 0$. This limit is set to $p \times \mathrm{DCA} < 350$ cm$\times$GeV/c for tracks exiting the absorber within $17.6 < R_{\rm abs} < 26.5$ cm, and $p \times \mathrm{DCA} < 200$ cm$\times$GeV/c for those within $26.5 < R_{\rm abs} < 89.5$ cm.

The purity of selected event candidates is ensured by applying a veto on the total FV0 signal amplitude in the bunch crossing associated with the reconstructed muon tracks. The presence of residual hadronic or electromagnetic pileup from multiple interactions per bunch crossing may result in rejection of signal events due to the FV0 veto requirement. This probability is defined as the veto inefficiency, $P_{\rm FV0}$. For the analyzed data periods with a typical interaction rate of 30 to 50 kHz, the probability of hadronic pileup did not exceed 0.35%. The veto inefficiency is estimated to be below 0.4% based on an analysis of FV0 signals from an unbiased sample of bunch crossings, selected without any additional detector requirements. The veto efficiency correction factor is estimated as a weighted average across all data-taking periods, using the corresponding integrated luminosities as weights, and is found to be $\varepsilon_{\rm veto} = 1 - P_{\rm FV0} = 99.8\%$. The associated uncertainty is discussed in section 3.1.

To estimate the dimuon reconstruction efficiency and model the invariant mass and transverse momentum distributions, the analysis utilizes a Monte Carlo-based full detector simulation within the ALICE O^2 framework [71] that incorporates the continuous readout regime and a detailed description of time-dependent detector conditions for all data-taking periods. Large samples generated with STARlight 2.2 [39, 40] are used to simulate coherent and incoherent photoproduction of J/ψ and ψ(2S) mesons, including the feed-down process $\psi(2\mathrm{S}) \to \mathrm{J}/\psi + \pi\pi$. For the feed-down, J/$\psi$ mesons are simulated assuming that they inherit

JHEP10(2026)057

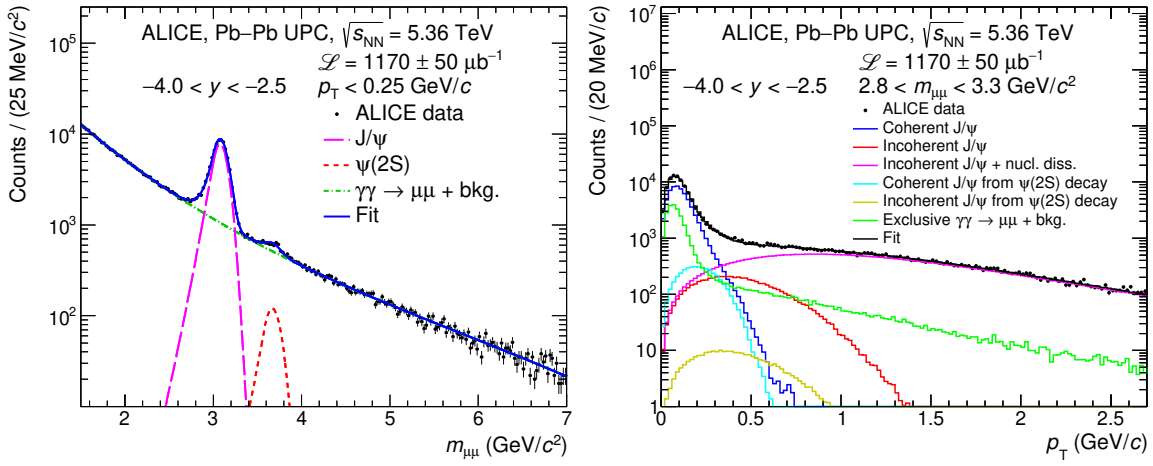


Figure 2. Left: invariant mass distribution for the selected muon pairs with $p_{\mathrm{T}} < 0.25$ GeV/c in the full forward rapidity range. Right: transverse momentum distribution for muon pairs in the invariant mass range $2.8 < m_{\mu\mu} < 3.3$ GeV/c^2. Fit components are described in the text.

the transverse polarization from the primary ψ(2S), according to previous measurements [72, 73]. Exclusive dimuon production is modeled with the Upcgen generator [44, 45].

The J/ψ and ψ(2S) yields are measured in six and two rapidity intervals, respectively. Figure 2, left, shows the invariant mass distribution for the muon pairs in the full forward rapidity range after applying a selection on the dimuon transverse momentum $p_{\mathrm{T}} < 0.25$ GeV/c that is imposed to suppress incoherent and background events. The fit to the mass distribution is used to extract raw inclusive J/ψ and ψ(2S) yields, as well as the raw yield for the exclusive $\gamma\gamma \to \mu\mu$ process. The shape of the non-resonant dimuon distribution is modeled with an exponential function [74]. The peaks associated with the J/ψ and ψ(2S) mesons are fitted using double-sided Crystal Ball functions [74, 75]. For each individual rapidity interval, the tail parameters of the Crystal Ball functions are fixed to the values obtained from the realistic simulations. The mass and width parameters of the J/ψ distributions are left unconstrained, while the ψ(2S) mass parameter is connected to the J/ψ one according to the mass difference between the two resonances obtained from the PDG [76]. Based on the ratio of their widths evaluated in simulations, the ψ(2S) width parameter is fixed to the J/ψ width multiplied by a factor of 1.1.

The fit to the invariant mass distribution shown in figure 2, left, is also used to obtain the ratio of raw inclusive ψ(2S) and J/ψ yields, $N_{\psi(2S)}$ and $N_{\mathrm{J}/\psi}$:

$$R_N = \frac{N_{\psi(2S)}}{N_{\mathrm{J}/\psi}} = 0.017 \pm 0.002\,(\mathrm{stat.})^{+0.001}_{-0.002}\,(\mathrm{syst.})\,. \tag{3.1}$$

The associated systematic uncertainty is discussed in section 3.1. The measured ratio R_N is then used to obtain the fraction of feed-down J/ψ in the raw inclusive J/ψ yield:

$$R_{\mathrm{fd}} = \frac{N^{\mathrm{feed-down}}_{\mathrm{J}/\psi}}{N_{\mathrm{J}/\psi}} = \frac{(BR \times \varepsilon)_{\psi(2S)\to \mathrm{J}/\psi + X \to \mu\mu + X}}{(BR \times \varepsilon)_{\psi(2S)\to\mu\mu}} \times R_N, \tag{3.2}$$

where $(BR \times \varepsilon)$ is the product of the branching ratio and reconstruction efficiency for the corresponding process. The reconstruction efficiencies were obtained using STARlight-based

JHEP10(2026)057

simulations: $\varepsilon(\mathrm{J}/\psi \to \mu\mu) = 21\%$ and $\varepsilon(\psi(2\mathrm{S}) \to \mathrm{J}/\psi + X \to \mu\mu + X) = 13\%$ for the full forward rapidity range. The following branching ratios were used [76]: $BR(\psi(2\mathrm{S}) \to \mathrm{J}/\psi + X) = (61.5 \pm 0.7)\%$, $BR(\mathrm{J}/\psi \to \mu\mu) = (5.961 \pm 0.033)\%$, $BR(\psi(2\mathrm{S}) \to \mu\mu) = (0.80 \pm 0.06)\%$.

The R_{fd} ratio is then used to extract the fraction of feed-down J/ψ relative to the primary J/ψ yield:

$$f_{\mathrm{D}} = \frac{N_{\mathrm{J}/\psi}^{\mathrm{feed-down}}}{N_{\mathrm{J}/\psi}^{\mathrm{primary}}} = \frac{N_{\mathrm{J}/\psi}^{\mathrm{feed-down}}}{N_{\mathrm{J}/\psi} - N_{\mathrm{J}/\psi}^{\mathrm{feed-down}}} = (1/R_{\mathrm{fd}} - 1)^{-1}\,. \tag{3.3}$$

The feed-down fraction $f_{\mathrm{D}} = (4.9^{+0.5}_{-0.6})\%$ is obtained for dimuon $p_{\mathrm{T}} < 0.25$ GeV/c in the full forward rapidity range. This feed-down fraction value is then used in all rapidity intervals, assuming a weak rapidity dependence, as suggested by theoretical studies of coherent J/ψ and $\psi(2\mathrm{S})$ photoproduction in Pb–Pb UPCs [9].

The inclusive J/ψ yields extracted from the mass fits contain contributions from both the coherent and incoherent photoproduction. In order to account for the remaining incoherent J/ψ contamination for $p_{\mathrm{T}} < 0.25$ GeV/c, the p_{T} distribution in the dimuon invariant mass range $2.8 < m_{\mu\mu} < 3.3$ GeV/c^2 is fitted with templates prepared for all the processes using the simulations mentioned above, with two exceptions. For the exclusive dimuon production, side-band templates are prepared with the p_{T} distributions from adjacent mass regions without a charmonium signal. High-p_{T} contribution in the distributions, associated with incoherent J/ψ photoproduction accompanied by nucleon dissociation, is modeled with templates based on the H1 parametrization [77]:

$$\frac{\mathrm{d}N}{\mathrm{d}p_{\mathrm{T}}} \propto p_{\mathrm{T}} \left(1 + \frac{b_{\mathrm{pd}}}{n_{\mathrm{pd}}} p_{\mathrm{T}}^2\right)^{-n_{\mathrm{pd}}}\,. \tag{3.4}$$

In the rapidity-differential analysis, the H1 parameters are fitted in each rapidity interval individually. As an illustrative example, the fit performed over the full forward rapidity range yields $b_{\mathrm{pd}} = 0.81$ (GeV/c)$^{-2}$ and $n_{\mathrm{pd}} = 3.33$. The normalizations of the coherent and incoherent J/ψ components are left as free parameters, while the exclusive dimuon template is scaled to match the yield from the invariant mass fit. The feed-down J/ψ contribution is scaled relative to the primary J/ψ templates by the f_{D} fraction previously determined from the invariant mass fits in the full forward rapidity range.

The fit to the p_{T} distribution in the full forward rapidity range is shown in figure 2, right. The extracted contribution of the incoherent photoproduction processes, defined as $f_{\mathrm{I}} = N_{\mathrm{J}/\psi}^{\mathrm{incoh}}/N_{\mathrm{J}/\psi}^{\mathrm{coh}}$, ranges from 3.7% to 5.9% for $p_{\mathrm{T}} < 0.25$ GeV/c depending on the rapidity interval. The absolute value of the related systematic uncertainty varies from -0.2% to $+1.5\%$, as discussed in section 3.1. The same f_{I} values are used to estimate the incoherent $\psi(2\mathrm{S})$ fraction in the raw $\psi(2\mathrm{S})$ yields, assuming a similar incoherent-to-coherent ratio for $\psi(2\mathrm{S})$ and J/ψ [78, 79].

Raw exclusive dimuon production yields are extracted in five invariant mass intervals, ranging from 1.5 to 10 GeV/c^2, within three equal rapidity intervals. The extracted yields include several components: the exclusive dimuon production; the incoherent $\gamma\gamma \to \mu\mu$ process [80], in which at least one of the photons is emitted inelastically by the nucleus, resulting in nuclear excitation or breakup; contamination induced by beam-gas interactions

JHEP10(2026)057

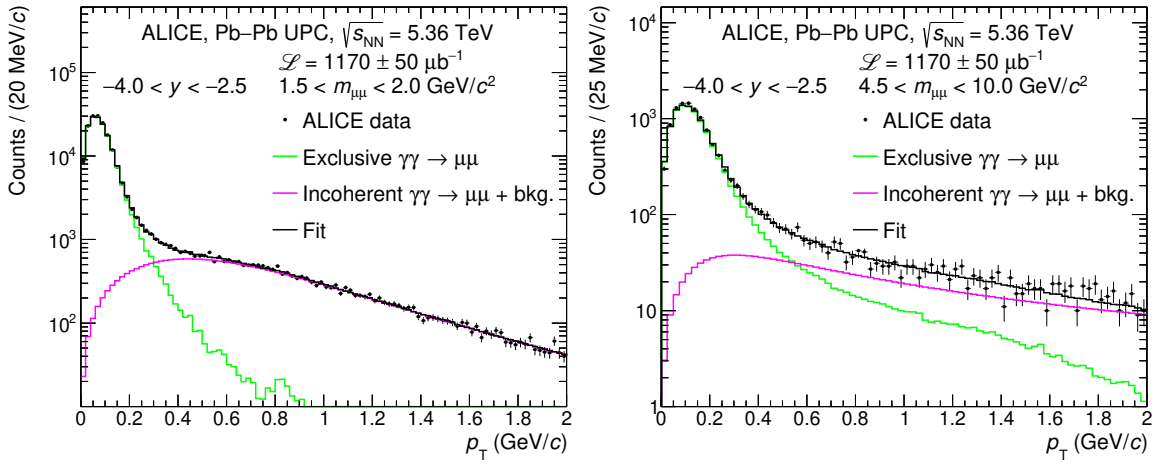


Figure 3. Transverse momentum distribution for muon pairs in the full rapidity range for two invariant mass intervals. Fit components are described in the text.

and potential contamination from peripheral hadronic collisions that pass the veto requirement (discussed in section 3.1). The exclusive $\gamma\gamma \to \mu\mu$ signal yields, as well as the fraction of the background contributions mentioned above $f_{\mathrm{I}}^{\gamma\gamma} = N_{\mu\mu}^{\mathrm{background}}/N_{\mu\mu}^{\mathrm{exclusive}}$, are estimated by fitting the dimuon transverse momentum distributions in the invariant mass intervals, excluding the range $2.5 < m_{\mu\mu} < 4.5$ GeV/c^2 with the contribution from the J/ψ and ψ(2S) resonances. The fit utilizes the Upcgen template for the exclusive $\gamma\gamma \to \mu\mu$ and the H1 parametrization (eq. (3.4)) for the background. To reproduce the broadening of the low-p_{T} component associated with the exclusive $\gamma\gamma \to \mu\mu$, a scaling factor for the width of the Upcgen template is included as a free parameter in the fit. Figure 3 shows the resulting fits for the full rapidity range in the lowest and highest invariant mass intervals. The extracted background fraction ranges from 1.9% to 6.4% depending on the mass and rapidity interval, with the absolute systematic uncertainty varying from −1.0% to +0.6%. In the J/ψ and ψ(2S) invariant mass regions, a side-band method is applied where the $f_{\mathrm{I}}^{\gamma\gamma}$ factor is averaged over adjacent mass intervals without a charmonia signal.

3.1 Systematic uncertainties

A summary of systematic uncertainties assessed in this analysis is presented in table 1.

The 4.3% uncertainty on the luminosity is the quadrature sum of three components: a 3.2% uncertainty from the inelastic cross section measurement at $\sqrt{s_{\mathrm{NN}}} = 5.02$ TeV [63], a 2.0% uncertainty from the FT0 centrality determination evaluated by varying the Glauber fit anchor point, and a 2.0% uncertainty from the variation observed when using ZDC-based triggers.

The production of vector mesons and muon pairs in peripheral heavy-ion collisions, previously observed by ALICE [81, 82], can contaminate the UPC raw yields at the level of a few percent when the associated hadronic activity is not rejected by the FV0 veto. To estimate the magnitude of this effect, the FV0 signal threshold is varied within limits corresponding to a few percent change in the centrality of the observed collisions. The uncertainty associated with the veto efficiency is estimated to be 1% for J/ψ, ψ(2S), and the exclusive dimuon production.

JHEP10(2026)057

Source	$\sigma(\mathrm{J}/\psi)$	$\sigma(\psi(2\mathrm{S}))$	$\sigma(\psi(2\mathrm{S}))/\sigma(\mathrm{J}/\psi)$	$\sigma(\gamma\gamma \to \mu\mu)$
Luminosity	± 4.3	± 4.3	—	± 4.3
Veto	± 1.0	± 1.0	—	± 1.0
Tracking	± 3.0	± 3.0	—	± 3.0
Matching	$+7.3$	$+6.1$	—	$+21.8$
Signal extraction	$-1.1, +1.5$	$-10.2, +5.6$	$-10.2, +5.8$	$-2.3, +1.4$
Incoherent/background fraction	$-1.5, +0.1$	$-0.8, +0.1$	$-1.7, +0.2$	$-0.6, +1.0$
Feed-down fraction	$-0.5, +0.6$	—	$-0.5, +0.6$	—
Branching ratio	± 0.6	± 7.5	± 7.5	—
Total	$-5.3, +9.0$	$-13.6, +12.3$	$-12.8, +9.5$	$-5.5, +22.4$

Table 1. Summary of the relative systematic uncertainties, shown in percent. When two values are quoted, they correspond to the negative and positive variations obtained in the given rapidity and invariant mass intervals. The values reported in the table are the extrema of these variations observed across the analyzed intervals. Uncertainties quoted as '±' are symmetric and are taken to be identical for all intervals. Luminosity estimation, veto efficiency, and branching ratio uncertainties are fully correlated versus rapidity. All other sources of uncertainty are considered partially correlated across different rapidity and invariant mass intervals.

The uncertainty of 3% associated with the MCH tracking pseudo-efficiency stems from the accuracy of the detector description implemented in the simulation. It is extracted from comparing single-muon tracking pseudo-efficiency values obtained from simulation and data, with a procedure based on the redundancy of the tracking-chamber information, as described in ref. [83].

The systematic uncertainty on the efficiency of the MCH-MID matching originates from the evaluation of the intrinsic efficiencies of MID chambers, the algorithm used for the reconstruction of MID track segments, and the MCH-MID matching algorithm. The baseline analysis is performed using a dataset of event candidates consisting of two MCH-MID tracks. The MCH-MID matching uncertainty is evaluated using the corrected exclusive yields from event samples requiring one MCH-MID track matched to another MCH track within a ±10 BC interval. The resulting uncertainty is below 7.3% for J/ψ, 6.1% for $\psi(2\mathrm{S})$, and 21.8% for exclusive dimuon production. The largest uncertainties are observed at low rapidities for J/ψ and $\psi(2\mathrm{S})$, and at low rapidities and low invariant masses for the exclusive dimuon production.

The uncertainties related to the J/ψ and $\psi(2\mathrm{S})$ signal extraction are estimated by performing invariant mass fits with different configurations. The lower limit of the fit is varied from 1.5 to 2.5 GeV/c^2, and the upper limit is varied from 5 to 7 GeV/c^2. Different fitting functions for the non-resonant background are tested: the product of an exponential function and a fourth-order polynomial, an exponential function, and a variable-width Gaussian function [74]. In addition, the $\psi(2\mathrm{S})$-to-J/ψ width ratio obtained from the simulations

JHEP10(2026)057

is varied by ±0.1 based on the expected resolution in the reconstructed invariant mass of the vector mesons. To further test the invariant mass fits, the J/ψ and ψ(2S) yields are compared to the case when the tail parameters of the Crystal Ball functions are left unconstrained. The same procedure is used for the uncertainty related to the extraction of the $\gamma\gamma \to \mu\mu$ contribution in the J/ψ and ψ(2S) regions. In addition, the limits on the transverse momentum of the single muon and the value of $p \times$ DCA, used for the track selection, are varied in all kinematic regions and for all the processes. The resulting signal extraction systematic uncertainties vary from −1.1% to +1.5% for J/ψ, from −10.2% to +5.6% for ψ(2S), and from −2.3% to +1.4% for the exclusive dimuon production depending on the mass and rapidity interval. The uncertainties are asymmetric in each interval, and the quoted values represent the lowest and the highest variations observed across all intervals. For charmonia, the dominant contribution to the signal extraction uncertainty originates from the choice of the background function, while for the exclusive dimuon production, the main source of uncertainty is due to variation of the $p \times$ DCA selection criterion.

In order to estimate systematic uncertainties associated with p_{T} template fits, several tests are performed. For the J/ψ analysis, systematic tests include varying the invariant mass range for the transverse momentum fits (with the lower limit varied between 2.5 and 2.8 GeV/c^2 and the upper one between 3.2 and 3.5 GeV/c^2), and varying the single-muon selection criteria for transverse momentum and $p \times$ DCA. The uncertainty associated with extracting the incoherent and background fractions is estimated to be between −1.5% and +0.1% for J/ψ, and between −0.8% to +0.1% for ψ(2S). For the exclusive dimuon production, the variations result in an uncertainty ranging from −0.6% to +1.0% depending on the rapidity and invariant mass interval.

An additional uncertainty arises from the p_{T} fitting procedure due to the estimation of the feed-down J/ψ fraction, affecting both the J/ψ cross section and the ψ(2S)-to-J/ψ yield ratio. The feed-down fraction f_{D} is varied from 4.3% to 5.4%, based on the systematic uncertainty of the ψ(2S)-to-J/ψ yield ratio (eq. (3.1)) and the associated branching ratio uncertainties (eq. (3.2)). This variation leads to an uncertainty ranging from −0.5% to +0.6%, depending on the rapidity interval.

Variations of the generated rapidity distributions in the simulations are found to have a negligible impact on the corrected yields, and therefore, this contribution is not included in the uncertainty evaluation. Possible migrations between neighboring rapidity and invariant-mass intervals due to detector resolution are also found to be negligible.

The checks relevant to the J/ψ and ψ(2S) analyses are repeated for the measurement of the ψ(2S)-to-J/ψ cross section ratio. The uncertainties arising from the ψ(2S) signal extraction are found to be dominant. The uncertainties stemming from the luminosity determination, veto efficiency estimates, evaluation of the MCH tracking and MCH-MID matching efficiencies largely cancel in the ratio measurement.

JHEP10(2026)057

Rapidity	$N_{J/\psi}$	ε_{rec} (%)	f_I	$d\sigma/dy$ (mb)
$(-4.00, -2.50)$	67548 ± 346	21	0.052	2.78 ± 0.01 (stat.) $^{+0.19}_{-0.15}$ (syst.)
$(-4.00, -3.75)$	2471 ± 61	6.8	0.059	1.89 ± 0.05 (stat.) $^{+0.11}_{-0.10}$ (syst.)
$(-3.75, -3.50)$	9578 ± 123	22	0.058	2.28 ± 0.03 (stat.) $^{+0.13}_{-0.12}$ (syst.)
$(-3.50, -3.25)$	18577 ± 180	36	0.053	2.67 ± 0.03 (stat.) $^{+0.16}_{-0.15}$ (syst.)
$(-3.25, -3.00)$	20057 ± 190	35	0.051	2.97 ± 0.03 (stat.) $^{+0.24}_{-0.16}$ (syst.)
$(-3.00, -2.75)$	13081 ± 153	22	0.041	3.20 ± 0.04 (stat.) $^{+0.26}_{-0.17}$ (syst.)
$(-2.75, -2.50)$	3586 ± 83	5.6	0.037	3.38 ± 0.08 (stat.) $^{+0.31}_{-0.19}$ (syst.)

Table 2. Raw J/ψ yields with their statistical uncertainties, J/ψ reconstruction efficiencies, f_I fractions, and coherent cross sections.

Rapidity	$N_{\psi(2S)}$	ε_{rec} (%)	f_I	$d\sigma/dy$ (mb)
$(-4.00, -2.50)$	1164 ± 105	22	0.052	0.36 ± 0.03 (stat.) $^{+0.04}_{-0.04}$ (syst.)
$(-4.00, -3.25)$	503 ± 66	24	0.056	0.29 ± 0.04 (stat.) $^{+0.03}_{-0.04}$ (syst.)
$(-3.25, -2.50)$	638 ± 81	20	0.047	0.43 ± 0.05 (stat.) $^{+0.05}_{-0.04}$ (syst.)

Table 3. Raw ψ(2S) yields with their statistical uncertainties, ψ(2S) reconstruction efficiencies, f_I fractions and coherent cross sections.

4 Results and discussion

4.1 Coherent J/ψ and ψ(2S) cross sections

The rapidity-differential cross section of coherent J/ψ and ψ(2S) is obtained for a given rapidity interval Δy with

$$\frac{d\sigma_{VM}^{coh}}{dy} = \frac{N_{VM}^{excl}}{\varepsilon_{rec}\varepsilon_{veto} BR(VM \to \mu\mu)\mathcal{L}\Delta y}, \tag{4.1}$$

where ε_{rec} denotes the reconstruction efficiency of the produced vector meson VM, and N_{VM}^{excl} is the estimated exclusive yield that can be obtained from the corresponding raw yield with $N_{VM}^{excl} = N_{J/\psi}/(1 + f_I + f_D)$ for the coherent J/ψ and with $N_{VM}^{excl} = N_{\psi(2S)}/(1 + f_I)$ for the coherent ψ(2S), respectively. The raw J/ψ and ψ(2S) yield values, reconstruction efficiencies, f_I fractions, and coherent J/ψ and ψ(2S) cross sections with corresponding statistical and systematic uncertainties are summarized in tables 2 and 3, respectively.

The results for coherent J/ψ and ψ(2S) cross sections as a function of rapidity are presented in figure 4 and are compared with theoretical predictions. The J/ψ measurements probe the gluon content of the nucleus at Bjorken-x values either in the range $1.1 \times 10^{-5} < x < 4.7 \times 10^{-5}$ or $0.7 \times 10^{-2} < x < 3.2 \times 10^{-2}$, depending on which nucleus emitted the photon. The corresponding Bjorken-x ranges for ψ(2S) are $1.3 \times 10^{-5} < x < 5.6 \times 10^{-5}$ and $0.8 \times 10^{-2} < x < 3.8 \times 10^{-2}$.

JHEP10(2026)057

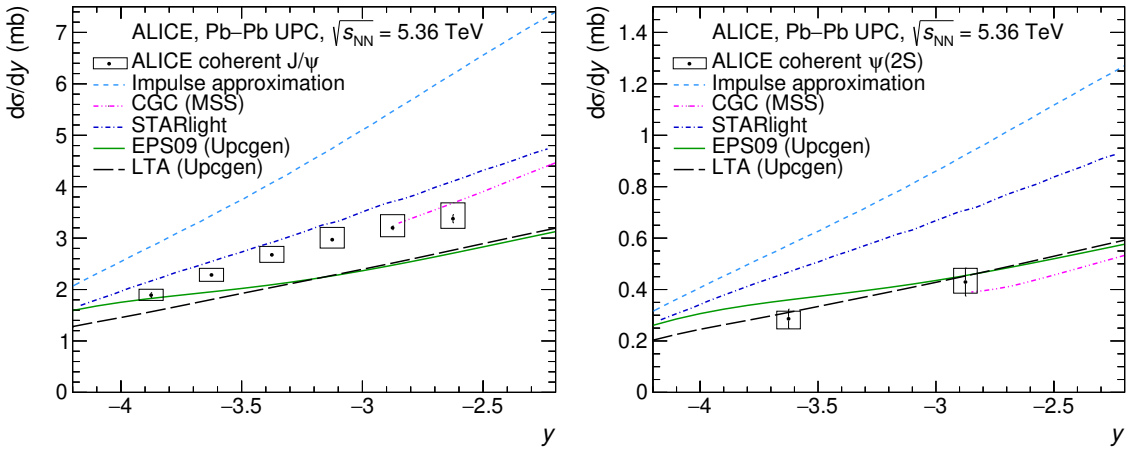


Figure 4. Measured rapidity-differential cross sections of the coherent J/ψ (left) and ψ(2S) (right) production in Pb–Pb UPCs at $\sqrt{s_{\rm NN}}$ = 5.36 TeV. The results are compared with theoretical calculations described in the text. The statistical uncertainties are shown with bars, the systematic uncertainties are shown with boxes.

The impulse approximation, taken from STARlight [39, 40, 84], is based on the HERA data for the exclusive J/ψ photoproduction off protons and neglects all nuclear effects except for coherence. The square root of the ratio of experimental points to the impulse approximation cross section is about 0.76 for J/ψ and 0.71 for ψ(2S), reflecting the magnitude of the nuclear gluon shadowing factor at $y \approx -3$ corresponding to typical Bjorken-x values around 10^{-2}, under the assumption that the contribution from low Bjorken-x values $\sim 10^{-5}$ can be neglected [8].

STARlight predictions for coherent vector meson cross sections in Pb–Pb UPCs are based on the Vector Meson Dominance model for the conversion of photons into vector mesons and a Glauber-like formalism to account for multiple scattering effects. STARlight overpredicts both the J/ψ and ψ(2S) cross sections, with a larger discrepancy for the latter, suggesting that the observed suppression of the coherent vector meson cross sections cannot be fully explained by Glauber-like rescatterings alone, and other effects, such as gluon shadowing, must be considered.

Gluon shadowing effects are taken into account explicitly in the predictions from the Upcgen generator [44, 45] that is based on the leading-order perturbative QCD approach introduced in ref. [9]. Two gluon shadowing models are considered: the first is based on the EPS09 LO parametrization of the available nuclear shadowing data [10] (EPS09) and the other on the leading twist approximation (LTA) of nuclear shadowing [11] with the weak shadowing scenario. The Upcgen predictions are found to be in good agreement with ψ(2S) cross section measurements. However, both shadowing models lie below the measured J/ψ cross section in the range $-3.75 < y < -2.5$.

Predictions from Mäntysaari, Salazar, and Schenke (MSS) are based on the color glass condensate (CGC) implementation of saturation effects accounting for event-by-event fluctuations of the nucleon substructure in heavy nuclei [12]. The model is only valid for Bjorken-x smaller than 10^{-2} corresponding to $|y| < 2.85$. Within this domain, the model predictions

JHEP10(2026)057

Rapidity	$\sigma(\psi(2S))/\sigma(J/\psi)$
$(-4.00, -2.50)$	0.131 ± 0.012 (stat.) $^{+0.013}_{-0.013}$ (syst.)
$(-4.00, -3.25)$	0.124 ± 0.016 (stat.) $^{+0.011}_{-0.016}$ (syst.)
$(-3.25, -2.50)$	0.132 ± 0.017 (stat.) $^{+0.015}_{-0.011}$ (syst.)

Table 4. Ratio of coherent J/ψ and ψ(2S) cross sections in three rapidity intervals.

agree with the measured J/ψ and ψ(2S) cross sections. In addition, the model provides a reasonable description of the recent ATLAS measurements at $\sqrt{s_{\rm NN}} = 5.36$ TeV [30], although some tension remains between the ATLAS results and ALICE midrapidity measurements at $\sqrt{s_{\rm NN}} = 5.02$ TeV [18].

The obtained results can be compared with the previous measurement performed by ALICE in the same rapidity region in Pb–Pb UPCs at $\sqrt{s_{\rm NN}} = 5.02$ TeV [16]. The reported value for the coherent J/ψ cross section measured across the full rapidity interval is $2.549 \pm 0.022(\text{stat.})^{+0.209}_{-0.237}(\text{syst.})$ mb, which is 9% lower than the value reported in this Paper. This difference is consistent, within the experimental uncertainties, with theoretical expectations based on STARlight's implementation of the impulse approximation, which predicts a 6–11% increase depending on the rapidity interval.

The ψ(2S)-to-J/ψ cross section ratio in the full forward rapidity range and in two rapidity intervals is presented in table 4. The measured ψ(2S)-to-J/ψ cross section ratio agrees within 1.1σ with previous ALICE [16] and LHCb [27] measurements at forward rapidity in Pb–Pb UPCs at $\sqrt{s_{\rm NN}} = 5.02$ TeV: $R = 0.150 \pm 0.018(\text{stat.}) \pm 0.021(\text{syst.}) \pm 0.007(\text{BR})$ and $R = 0.155 \pm 0.014(\text{stat.}) \pm 0.003(\text{syst.})$, respectively.

Figure 5 compares the measured ratio with theoretical predictions. The CGC-based model is consistent with the measurement within its validity range. The impulse approximation, which uses the ψ(2S)-to-J/ψ cross section ratio $R = 0.166 \pm 0.007(\text{stat.}) \pm 0.008(\text{syst.}) \pm 0.007(\text{BR})$ measured by the H1 collaboration [78], lies above the ALICE data but remains compatible within 1.9σ in the rapidity interval $-4 < y < -3.25$ and within 1.4σ in the interval $-3.25 < y < -2.5$. The STARlight, LTA, and EPS09 models predict nearly identical cross section ratios, differing by less than 0.01 and lying slightly above the impulse approximation prediction. All these predictions remain compatible with the data within the present uncertainties.

4.2 Cross section of exclusive dimuon production

The invariant mass-differential cross section for the exclusive dimuon production is extracted for a given invariant mass Δm as follows

$$\frac{\mathrm{d}\sigma^{\rm excl}_{\gamma\gamma\to\mu\mu}}{\mathrm{d}m_{\mu\mu}} = \frac{N_{\gamma\gamma\to\mu\mu}}{(1+f_{\rm I}^{\gamma\gamma})\varepsilon_{\rm rec}\varepsilon_{\rm veto}\mathcal{L}\Delta m} \,. \tag{4.2}$$

The raw $\gamma\gamma \to \mu\mu$ yield values, reconstruction efficiencies $\varepsilon_{\rm rec}$, $f_{\rm I}^{\gamma\gamma}$ fractions, and the resulting cross sections with corresponding statistical and systematic uncertainties are summarized in table 5 for four rapidity ranges.

JHEP10(2026)057

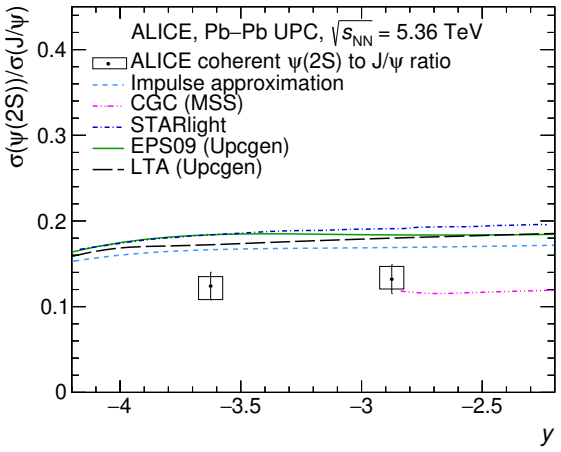


Figure 5. Measured ratio of differential photoproduction cross sections of the coherent J/ψ and ψ(2S) in Pb–Pb UPCs at $\sqrt{s_{\rm NN}}$ = 5.36 TeV. The results are compared with theoretical calculations described in the text. The statistical uncertainties are shown as bars, the systematic uncertainties are shown as boxes.

Figure 6 compares the measured exclusive dimuon production cross sections to predictions from the Upcgen [44, 45], SuperChic 4 [42, 43], and STARlight [39, 40] generators. STARlight calculates photon fluxes assuming point-like sources with a hard cutoff at the nuclear radius, while Upcgen and SuperChic 4 model photon fluxes using nuclear form factors, which account for photon emission from within the nucleus. This difference leads to higher predicted cross sections in Upcgen and SuperChic 4 compared to STARlight, particularly at high invariant masses and large rapidities, where photon emission at small impact parameters becomes more important.

STARlight predictions agree with the measured cross sections in the lowest rapidity range $-3.0 < y < -2.5$. However, at higher rapidities, STARlight underestimates the measured exclusive dimuon production cross section by as much as 40%, the deviation being more pronounced towards higher masses and rapidities. A similar trend is observed in the dimuon and dielectron production measurements at forward rapidity performed by ATLAS [48, 49]. In contrast to STARlight, both Upcgen and SuperChic 4 predictions are approximately 1–2σ higher than the data, across all invariant mass intervals and rapidity ranges.

The comparison of the measured cross sections with model predictions highlights the importance of accurate modeling of photon fluxes within the equivalent photon approximation, particularly at high rapidities and invariant masses, where point-like and realistic flux descriptions diverge most significantly [44]. Furthermore, higher-order QED corrections may be significant, as indicated by theoretical studies [38, 53, 80], and further high-precision measurements are crucial for providing additional insights.

5 Conclusion

Rapidity-differential measurements of the cross sections for the coherent J/ψ and ψ(2S) vector meson photoproduction at forward rapidity in Pb–Pb UPCs at $\sqrt{s_{\rm NN}}$ = 5.36 TeV were presented and compared with theoretical models. The impulse approximation significantly

JHEP10(2026)057

Rapidity	$m_{\mu\mu}$ (GeV/c^2)	$N_{\gamma\gamma\to\mu\mu}$	$\varepsilon_{\rm rec}$ (%)	$f_{\rm I}^{\gamma\gamma}$	dσ/dm (mb/GeV/c^2)
$(-4.0, -2.5)$	$(1.5, 2.0)$	166809 ± 408	4.9	0.024	5.700 ± 0.014 (stat.) $^{+0.888}_{-0.308}$ (syst.)
	$(2.0, 2.5)$	71565 ± 268	5.4	0.031	2.213 ± 0.008 (stat.) $^{+0.169}_{-0.119}$ (syst.)
	$(2.5, 3.5)$	50661 ± 225	5.4	0.034	0.780 ± 0.003 (stat.) $^{+0.048}_{-0.041}$ (syst.)
	$(3.5, 4.5)$	15019 ± 123	5.1	0.034	0.242 ± 0.002 (stat.) $^{+0.015}_{-0.013}$ (syst.)
	$(4.5, 10.0)$	9329 ± 97	4.4	0.037	0.0321 ± 0.0003 (stat.) $^{+0.0023}_{-0.0019}$ (syst.)
$(-4.0, -3.5)$	$(1.5, 2.0)$	35492 ± 188	4.6	0.033	1.286 ± 0.007 (stat.) $^{+0.076}_{-0.071}$ (syst.)
	$(2.0, 2.5)$	11848 ± 109	4.2	0.031	0.473 ± 0.004 (stat.) $^{+0.030}_{-0.025}$ (syst.)
	$(2.5, 3.5)$	7197 ± 85	3.9	0.047	0.152 ± 0.002 (stat.) $^{+0.009}_{-0.009}$ (syst.)
	$(3.5, 4.5)$	1804 ± 42	3.6	0.047	0.041 ± 0.001 (stat.) $^{+0.002}_{-0.002}$ (syst.)
	$(4.5, 10.0)$	837 ± 29	3.5	0.064	0.0035 ± 0.0001 (stat.) $^{+0.0002}_{-0.0002}$ (syst.)
$(-3.5, -3.0)$	$(1.5, 2.0)$	97296 ± 312	8.2	0.019	1.984 ± 0.006 (stat.) $^{+0.340}_{-0.107}$ (syst.)
	$(2.0, 2.5)$	42225 ± 205	9.2	0.024	0.769 ± 0.004 (stat.) $^{+0.057}_{-0.041}$ (syst.)
	$(2.5, 3.5)$	30105 ± 174	9.3	0.027	0.270 ± 0.002 (stat.) $^{+0.016}_{-0.014}$ (syst.)
	$(3.5, 4.5)$	8890 ± 94	9.0	0.027	0.083 ± 0.001 (stat.) $^{+0.005}_{-0.004}$ (syst.)
	$(4.5, 10.0)$	5351 ± 73	7.9	0.030	0.0102 ± 0.0001 (stat.) $^{+0.0007}_{-0.0006}$ (syst.)
$(-3.0, -2.5)$	$(1.5, 2.0)$	34021 ± 184	2.5	0.031	2.305 ± 0.012 (stat.) $^{+0.517}_{-0.126}$ (syst.)
	$(2.0, 2.5)$	17492 ± 132	3.1	0.046	0.919 ± 0.007 (stat.) $^{+0.087}_{-0.051}$ (syst.)
	$(2.5, 3.5)$	13519 ± 116	3.2	0.036	0.344 ± 0.003 (stat.) $^{+0.025}_{-0.018}$ (syst.)
	$(3.5, 4.5)$	4379 ± 66	3.1	0.036	0.115 ± 0.002 (stat.) $^{+0.009}_{-0.006}$ (syst.)
	$(4.5, 10.0)$	3141 ± 56	2.6	0.026	0.0182 ± 0.0003 (stat.) $^{+0.0015}_{-0.0011}$ (syst.)

Table 5. Raw exclusive dimuon production yields with their statistical uncertainties, reconstruction efficiencies, $f_{\rm I}^{\gamma\gamma}$ fractions and exclusive cross sections.

overestimates the data by a factor of 1.5–1.8, depending on the rapidity region, confirming the importance of gluon shadowing effects in the nucleus. Leading order pQCD calculations based on the EPS09 LO parametrization or the leading twist approximation give a reasonable description of the measured ψ(2S) cross sections, while underestimating the J/ψ data by 1–2σ. The CGC model agrees within its validity range $|y| < 2.85$, with both the measured J/ψ and ψ(2S) cross sections and the corresponding ratios.

Invariant-mass differential cross sections for the exclusive dimuon production at forward rapidity in Pb–Pb UPCs at $\sqrt{s_{\rm NN}} = 5.36$ TeV were presented and compared with predictions by Monte Carlo event generators in three rapidity regions. The STARlight model, which uses the point-like photon flux approximation, describes the data reasonably well in the $-3 < y < -2.5$ rapidity region, but underestimates the measurements at larger rapidities. Upcgen and SuperChic 4, on the other hand, yield consistently higher cross sections than the measured central values by about 1–2σ, across all invariant mass and rapidity intervals. The comparison with STARlight, Upcgen, and SuperChic 4 highlights the importance of accurate modeling of photon fluxes within the EPA framework.

JHEP10(2026)057

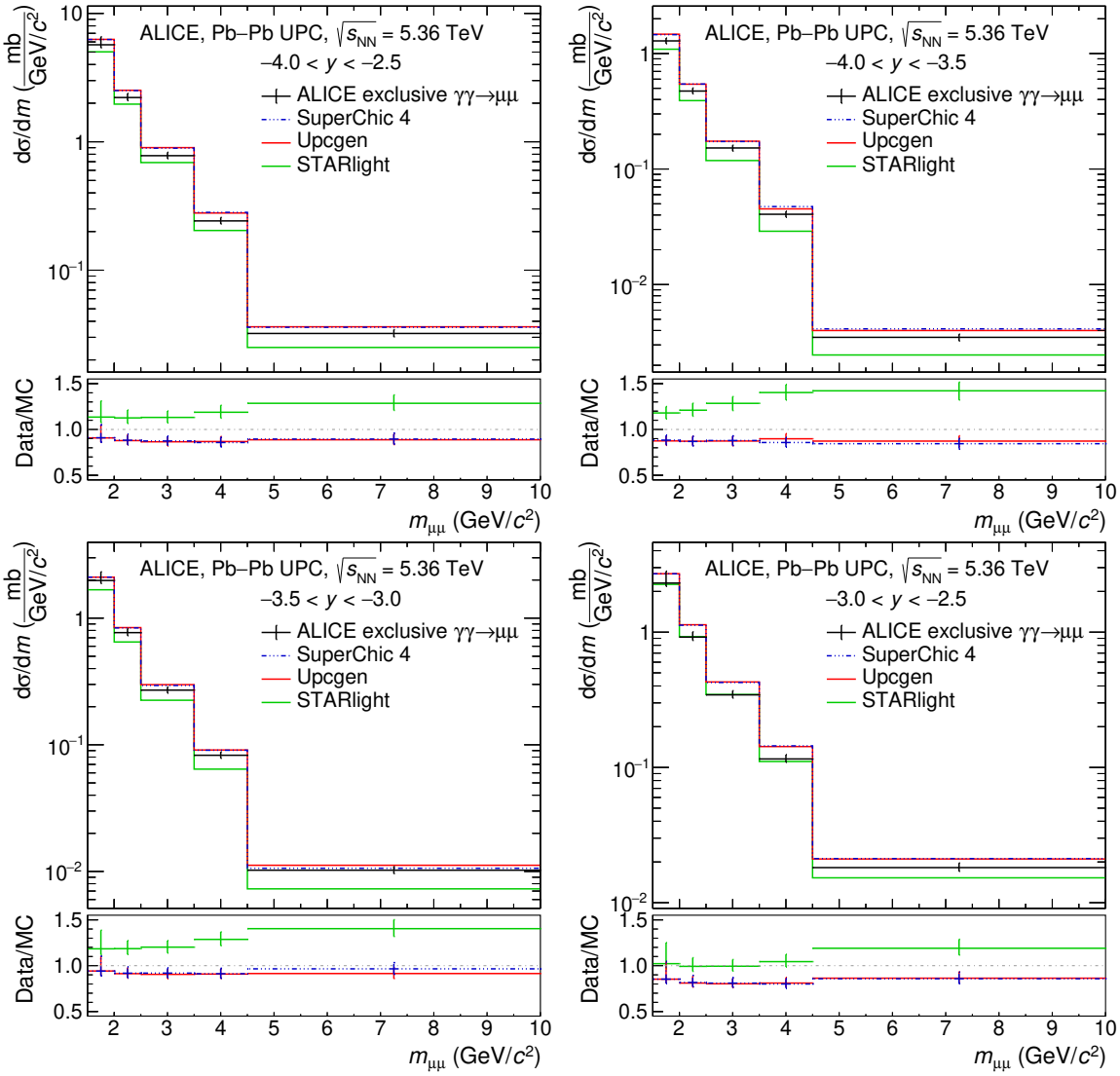


Figure 6. Measured invariant-mass differential cross sections of the exclusive dimuon production $\gamma\gamma \to \mu\mu$ in Pb–Pb UPCs at $\sqrt{s_{\rm NN}} = 5.36$ TeV. The results are compared with predictions by Monte Carlo generators [39, 40, 42–45] described in the text. The top part of the figures: the absolute values of the cross sections are presented. The bottom part of the figures: the ratios of data to Monte Carlo-based predictions are presented. The bars represent the total statistical and systematic uncertainty added in quadrature.

Future measurements of coherent heavy vector meson photoproduction with neutron emission at $\sqrt{s_{\rm NN}} = 5.36$ TeV will enable more detailed comparisons with theoretical predictions. Furthermore, additional high-precision data for the exclusive dilepton production are needed to further test available models and to investigate the potential relevance of higher-order effects.

JHEP10(2026)057

Acknowledgments

The ALICE Collaboration would like to thank all its engineers and technicians for their invaluable contributions to the construction of the experiment and the CERN accelerator teams for the outstanding performance of the LHC complex. The ALICE Collaboration gratefully acknowledges the resources and support provided by all Grid centres and the Worldwide LHC Computing Grid (WLCG) collaboration. The ALICE Collaboration acknowledges the following funding agencies for their support in building and running the ALICE detector: A.I. Alikhanyan National Science Laboratory (Yerevan Physics Institute) Foundation (ANSL), State Committee of Science and World Federation of Scientists (WFS), Armenia; Austrian Academy of Sciences, Austrian Science Fund (FWF): [M 2467-N36] and Nationalstiftung für Forschung, Technologie und Entwicklung, Austria; Ministry of Communications and High Technologies, National Nuclear Research Center, Azerbaijan; Rede Nacional de Física de Altas Energias (Renafae), Financiadora de Estudos e Projetos (Finep), Fundação de Amparo à Pesquisa do Estado de São Paulo (FAPESP) and The Sao Paulo Research Foundation (FAPESP), Brazil; Bulgarian Ministry of Education and Science, within the National Roadmap for Research Infrastructures 2020–2027 (object CERN), Bulgaria; Ministry of Education of China (MOEC), Ministry of Science & Technology of China (MSTC) and National Natural Science Foundation of China (NSFC), China; Ministry of Science and Education and Croatian Science Foundation, Croatia; Centro de Aplicaciones Tecnológicas y Desarrollo Nuclear (CEADEN), Cubaenergía, Cuba; Ministry of Education, Youth and Sports of the Czech Republic, Czech Republic; The Danish Council for Independent Research | Natural Sciences, the VILLUM FONDEN and Danish National Research Foundation (DNRF), Denmark; Helsinki Institute of Physics (HIP), Finland; Commissariat à l'Energie Atomique (CEA) and Institut National de Physique Nucléaire et de Physique des Particules (IN2P3) and Centre National de la Recherche Scientifique (CNRS), France; Bundesministerium für Forschung, Technologie und Raumfahrt (BMFTR) and GSI Helmholtzzentrum für Schwerionenforschung GmbH, Germany; National Research, Development and Innovation Office, Hungary; Department of Atomic Energy Government of India (DAE), Department of Science and Technology, Government of India (DST), University Grants Commission, Government of India (UGC) and Council of Scientific and Industrial Research (CSIR), India; National Research and Innovation Agency – BRIN, Indonesia; Istituto Nazionale di Fisica Nucleare (INFN), Italy; Japanese Ministry of Education, Culture, Sports, Science and Technology (MEXT) and Japan Society for the Promotion of Science (JSPS) KAKENHI, Japan; Consejo Nacional de Ciencia (CONACYT) y Tecnología, through Fondo de Cooperación Internacional en Ciencia y Tecnología (FONCICYT) and Dirección General de Asuntos del Personal Academico (DGAPA), Mexico; Nederlandse Organisatie voor Wetenschappelijk Onderzoek (NWO), Netherlands; The Research Council of Norway, Norway; Pontificia Universidad Católica del Perú, Peru; Ministry of Science and Higher Education, National Science Centre and WUT ID-UB, Poland; Korea Institute of Science and Technology Information and National Research Foundation of Korea (NRF), Republic of Korea; Ministry of Education and Scientific Research, Institute of Atomic Physics, Ministry of Research and Innovation and Institute of Atomic Physics and Universitatea Nationala de Stiinta si Tehnologie Politehnica Bucuresti, Romania; Ministerstvo skolstva, vyskumu, vyvoja a mladeze SR, Slovakia; National

JHEP10(2026)057

Research Foundation of South Africa, South Africa; Swedish Research Council (VR) and Knut & Alice Wallenberg Foundation (KAW), Sweden; European Organization for Nuclear Research, Switzerland; Suranaree University of Technology (SUT), National Science and Technology Development Agency (NSTDA) and National Science, Research and Innovation Fund (NSRF via PMU-B B05F650021), Thailand; Turkish Energy, Nuclear and Mineral Research Agency (TENMAK), Turkey; National Academy of Sciences of Ukraine, Ukraine; Science and Technology Facilities Council (STFC), United Kingdom; National Science Foundation of the United States of America (NSF) and United States Department of Energy, Office of Nuclear Physics (DOE NP), United States of America. In addition, individual groups or members have received support from: Czech Science Foundation (grant no. 23-07499S), Czech Republic; FORTE project, reg. no. CZ.02.01.01/00/22_008/0004632, Czech Republic, co-funded by the European Union, Czech Republic; European Research Council (grant nos. 101220549, 950692), European Union; Deutsche Forschungs Gemeinschaft (DFG, German Research Foundation) "Neutrinos and Dark Matter in Astro- and Particle Physics" (grant no. SFB 1258), Germany; CONVECS project, CUP C97H23001700002 FESR 2021-2027 program, Italy.

Data Availability Statement. This manuscript has associated data in a HEPData repository at: https://www.hepdata.net/record/ins3155120.

Code Availability Statement. This manuscript has associated code/software in a data repository. The code/software used for the analysis is publicly available on the github repository, at the link https://github.com/AliceO2Group/O2Physics.

Open Access. This article is distributed under the terms of the Creative Commons Attribution License (CC-BY4.0), which permits any use, distribution and reproduction in any medium, provided the original author(s) and source are credited.

References

[1] C.A. Bertulani, S.R. Klein and J. Nystrand, *Physics of ultra-peripheral nuclear collisions*, *Ann. Rev. Nucl. Part. Sci.* **55** (2005) 271 [nucl-ex/0502005] [INSPIRE].

[2] V. Guzey, M. Strikman and M. Zhalov, *Nucleon dissociation and incoherent J/ψ photoproduction on nuclei in ion ultraperipheral collisions at the Large Hadron Collider*, *Phys. Rev. C* **99** (2019) 015201 [arXiv:1808.00740] [INSPIRE].

[3] M.G. Ryskin, *Diffractive J/ψ electroproduction in LLA QCD*, *Z. Phys. C* **57** (1993) 89 [INSPIRE].

[4] A.L. Ayala, M.B. Gay Ducati and E.M. Levin, *QCD evolution of the gluon density in a nucleus*, *Nucl. Phys. B* **493** (1997) 305 [hep-ph/9604383] [INSPIRE].

[5] C.A. Flett et al., *How to include exclusive J/ψ production data in global PDF analyses*, *Phys. Rev. D* **101** (2020) 094011 [arXiv:1908.08398] [INSPIRE].

[6] K.J. Eskola et al., *Exclusive J/ψ photoproduction in ultraperipheral Pb+Pb collisions at the CERN Large Hadron Collider calculated at next-to-leading order perturbative QCD*, *Phys. Rev. C* **106** (2022) 035202 [arXiv:2203.11613] [INSPIRE].

JHEP10(2026)057

[7] C.A. Flett et al., *Exclusive vector-quarkonium photoproduction at NLO in αs in collinear factorisation with evolution of the generalised parton distributions and high-energy resummation*, *Phys. Lett. B* **859** (2024) 139117 [arXiv:2409.05738] [INSPIRE].

[8] V. Guzey, E. Kryshen, M. Strikman and M. Zhalov, *Evidence for nuclear gluon shadowing from the ALICE measurements of PbPb ultraperipheral exclusive J/ψ production*, *Phys. Lett. B* **726** (2013) 290 [arXiv:1305.1724] [INSPIRE].

[9] V. Guzey, E. Kryshen and M. Zhalov, *Coherent photoproduction of vector mesons in ultraperipheral heavy ion collisions: Update for run 2 at the CERN Large Hadron Collider*, *Phys. Rev. C* **93** (2016) 055206 [arXiv:1602.01456] [INSPIRE].

[10] K.J. Eskola, H. Paukkunen and C.A. Salgado, *EPS09: A New Generation of NLO and LO Nuclear Parton Distribution Functions*, *JHEP* **04** (2009) 065 [arXiv:0902.4154] [INSPIRE].

[11] L. Frankfurt, V. Guzey and M. Strikman, *Leading Twist Nuclear Shadowing Phenomena in Hard Processes with Nuclei*, *Phys. Rept.* **512** (2012) 255 [arXiv:1106.2091] [INSPIRE].

[12] H. Mäntysaari, F. Salazar and B. Schenke, *Energy dependent nuclear suppression from gluon saturation in exclusive vector meson production*, *Phys. Rev. D* **109** (2024) L071504 [arXiv:2312.04194] [INSPIRE].

[13] P. Newman and M. Wing, *The Hadronic Final State at HERA*, *Rev. Mod. Phys.* **86** (2014) 1037 [arXiv:1308.3368] [INSPIRE].

[14] ALICE collaboration, *Exclusive J/ψ photoproduction off protons in ultra-peripheral p-Pb collisions at $\sqrt{s_{\rm NN}} = 5.02$ TeV*, *Phys. Rev. Lett.* **113** (2014) 232504 [arXiv:1406.7819] [INSPIRE].

[15] ALICE collaboration, *Energy dependence of exclusive J/ψ photoproduction off protons in ultra-peripheral p–Pb collisions at $\sqrt{s_{\rm NN}} = 5.02$ TeV*, *Eur. Phys. J. C* **79** (2019) 402 [arXiv:1809.03235] [INSPIRE].

[16] ALICE collaboration, *Coherent J/ψ photoproduction at forward rapidity in ultra-peripheral Pb-Pb collisions at $\sqrt{s_{\rm NN}} = 5.02$ TeV*, *Phys. Lett. B* **798** (2019) 134926 [arXiv:1904.06272] [INSPIRE].

[17] ALICE collaboration, *First measurement of the $|t|$-dependence of coherent J/ψ photonuclear production*, *Phys. Lett. B* **817** (2021) 136280 [arXiv:2101.04623] [INSPIRE].

[18] ALICE collaboration, *Coherent J/ψ and ψ' photoproduction at midrapidity in ultra-peripheral Pb-Pb collisions at $\sqrt{s_{NN}} = 5.02$ TeV*, *Eur. Phys. J. C* **81** (2021) 712 [arXiv:2101.04577] [INSPIRE].

[19] ALICE collaboration, *The ALICE experiment: a journey through QCD*, *Eur. Phys. J. C* **84** (2024) 813 [arXiv:2211.04384] [INSPIRE].

[20] ALICE collaboration, *Exclusive and dissociative J/ψ photoproduction, and exclusive dimuon production, in p–Pb collisions at $\sqrt{s_{\rm NN}} = 8.16$ TeV*, *Phys. Rev. D* **108** (2023) 112004 [arXiv:2304.12403] [INSPIRE].

[21] ALICE collaboration, *Energy dependence of coherent photonuclear production of J/ψ mesons in ultra-peripheral Pb-Pb collisions at $\sqrt{s_{NN}} = 5.02$ TeV*, *JHEP* **10** (2023) 119 [arXiv:2305.19060] [INSPIRE].

[22] ALICE collaboration, *First measurement of the $|t|$-dependence of incoherent J/ψ photonuclear production*, *Phys. Rev. Lett.* **132** (2024) 162302 [arXiv:2305.06169] [INSPIRE].

JHEP10(2026)057

[23] ALICE collaboration, *Evidence for J/ψ suppression in incoherent photonuclear production*, *Phys. Rev. Lett.* **137** (2026) 052301 [arXiv:2503.18708] [INSPIRE].

[24] LHCb collaboration, *Exclusive J/ψ and $\psi(2S)$ production in pp collisions at $\sqrt{s} = 7$ TeV*, *J. Phys. G* **40** (2013) 045001 [arXiv:1301.7084] [INSPIRE].

[25] LHCb collaboration, *Updated measurements of exclusive J/ψ and $\psi(2S)$ production cross-sections in pp collisions at $\sqrt{s} = 7$ TeV*, *J. Phys. G* **41** (2014) 055002 [arXiv:1401.3288] [INSPIRE].

[26] LHCb collaboration, *Central exclusive production of J/ψ and $\psi(2S)$ mesons in pp collisions at $\sqrt{s} = 13$ TeV*, *JHEP* **10** (2018) 167 [arXiv:1806.04079] [INSPIRE].

[27] LHCb collaboration, *Study of exclusive photoproduction of charmonium in ultra-peripheral lead-lead collisions*, *JHEP* **06** (2023) 146 [arXiv:2206.08221] [INSPIRE].

[28] LHCb collaboration, *Measurement of exclusive J/ψ and $\psi(2S)$ production at $\sqrt{s} = 13$ TeV*, *SciPost Phys.* **18** (2025) 071 [arXiv:2409.03496] [INSPIRE].

[29] CMS collaboration, *Probing small Bjorken-x nuclear gluonic structure via coherent J/ψ photoproduction in ultraperipheral PbPb collisions at $\sqrt{s_N N} = 5.02$ TeV*, *Phys. Rev. Lett.* **131** (2023) 262301 [arXiv:2303.16984] [INSPIRE].

[30] ATLAS collaboration, *Measurement of coherent exclusive $J/\psi \to \mu^+\mu^-$ production in ultraperipheral Pb+Pb collisions at $\sqrt{s_{NN}} = 5.36$ TeV with the ATLAS detector*, *JHEP* **04** (2026) 020 [arXiv:2509.04135] [INSPIRE].

[31] STAR collaboration, *Exclusive J/ψ, $\psi(2s)$, and e^+e^- pair production in Au+Au ultra-peripheral collisions at RHIC*, *Phys. Rev. C* **110** (2024) 014911 [arXiv:2311.13632] [INSPIRE].

[32] STAR collaboration, *Observation of strong nuclear suppression in exclusive J/ψ photoproduction in Au+Au ultra-peripheral collisions at RHIC*, *Phys. Rev. Lett.* **133** (2024) 052301 [arXiv:2311.13637] [INSPIRE].

[33] PHENIX collaboration, *Photoproduction of J/ψ and of high mass e^+e^- in ultra-peripheral Au+Au collisions at $\sqrt{s} = 200$ GeV*, *Phys. Lett. B* **679** (2009) 321 [arXiv:0903.2041] [INSPIRE].

[34] G. Breit and J.A. Wheeler, *Collision of two light quanta*, *Phys. Rev.* **46** (1934) 1087 [INSPIRE].

[35] S. Klein, A.H. Mueller, B.-W. Xiao and F. Yuan, *Acoplanarity of a Lepton Pair to Probe the Electromagnetic Property of Quark Matter*, *Phys. Rev. Lett.* **122** (2019) 132301 [arXiv:1811.05519] [INSPIRE].

[36] S. Klein, A.H. Mueller, B.-W. Xiao and F. Yuan, *Lepton Pair Production Through Two Photon Process in Heavy Ion Collisions*, *Phys. Rev. D* **102** (2020) 094013 [arXiv:2003.02947] [INSPIRE].

[37] K. Hencken, E.A. Kuraev and V. Serbo, *Exclusive and inclusive muon pair production in collisions of relativistic nuclei*, *Phys. Rev. C* **75** (2007) 034903 [hep-ph/0606069] [INSPIRE].

[38] W. Zha and Z. Tang, *Discovery of higher-order quantum electrodynamics effect for the vacuum pair production*, *JHEP* **08** (2021) 083 [arXiv:2103.04605] [INSPIRE].

[39] A.J. Baltz, Y. Gorbunov, S.R. Klein and J. Nystrand, *Two-Photon Interactions with Nuclear Breakup in Relativistic Heavy Ion Collisions*, *Phys. Rev. C* **80** (2009) 044902 [arXiv:0907.1214] [INSPIRE].

[40] S.R. Klein et al., *STARlight: A Monte Carlo simulation program for ultra-peripheral collisions of relativistic ions*, *Comput. Phys. Commun.* **212** (2017) 258 [arXiv:1607.03838] [INSPIRE].

JHEP10(2026)057

[41] J.D. Jackson, *Classical electrodynamics*, 3rd edition, Wiley, New York U.S.A. (2021), [ISBN 9780471309321].

[42] L.A. Harland-Lang, V.A. Khoze and M.G. Ryskin, *Exclusive LHC physics with heavy ions: SuperChic 3*, *Eur. Phys. J. C* **79** (2019) 39 [arXiv:1810.06567] [INSPIRE].

[43] L.A. Harland-Lang, M. Tasevsky, V.A. Khoze and M.G. Ryskin, *A new approach to modelling elastic and inelastic photon-initiated production at the LHC: SuperChic 4*, *Eur. Phys. J. C* **80** (2020) 925 [arXiv:2007.12704] [INSPIRE].

[44] N. Burmasov, E. Kryshen, P. Buehler and R. Lavicka, *Upcgen: A Monte Carlo simulation program for dilepton pair production in ultra-peripheral collisions of heavy ions*, *Comput. Phys. Commun.* **277** (2022) 108388 [arXiv:2111.11383] [INSPIRE].

[45] N. Burmasov and E. Kryshen, *Update on Upcgen, an event generator for two-photon and photoproduction processes in ultraperipheral collisions*, *Int. J. Mod. Phys. E* **35** (2026) 2641023 [INSPIRE].

[46] ALICE collaboration, *Charmonium and e^+e^- pair photoproduction at mid-rapidity in ultra-peripheral Pb-Pb collisions at $\sqrt{s_{\rm NN}} = 2.76$ TeV*, *Eur. Phys. J. C* **73** (2013) 2617 [arXiv:1305.1467] [INSPIRE].

[47] CMS collaboration, *Observation of Forward Neutron Multiplicity Dependence of Dimuon Acoplanarity in Ultraperipheral Pb-Pb Collisions at $\sqrt{s_{NN}} = 5.02$ TeV*, *Phys. Rev. Lett.* **127** (2021) 122001 [arXiv:2011.05239] [INSPIRE].

[48] ATLAS collaboration, *Exclusive dimuon production in ultraperipheral Pb+Pb collisions at $\sqrt{s_{NN}} = 5.02$ TeV with ATLAS*, *Phys. Rev. C* **104** (2021) 024906 [arXiv:2011.12211] [INSPIRE].

[49] ATLAS collaboration, *Exclusive dielectron production in ultraperipheral Pb+Pb collisions at $\sqrt{s_{NN}} = 5.02$ TeV with ATLAS*, *JHEP* **06** (2023) 182 [arXiv:2207.12781] [INSPIRE].

[50] STAR collaboration, *Production of e^+e^- pairs accompanied by nuclear dissociation in ultra-peripheral heavy ion collision*, *Phys. Rev. C* **70** (2004) 031902 [nucl-ex/0404012] [INSPIRE].

[51] STAR collaboration, *Measurement of e^+e^- Momentum and Angular Distributions from Linearly Polarized Photon Collisions*, *Phys. Rev. Lett.* **127** (2021) 052302 [arXiv:1910.12400] [INSPIRE].

[52] L.A. Harland-Lang, V.A. Khoze and M.G. Ryskin, *Elastic photon-initiated production at the LHC: the role of hadron-hadron interactions*, *SciPost Phys.* **11** (2021) 064 [arXiv:2104.13392] [INSPIRE].

[53] H.-S. Shao and D. d'Enterria, *Dimuon and ditau production in photon-photon collisions at next-to-leading order in QED*, *JHEP* **02** (2025) 023 [arXiv:2407.13610] [INSPIRE].

[54] ALICE collaboration, *The ALICE experiment at the CERN LHC*, 2008 *JINST* **3** S08002 [INSPIRE].

[55] ALICE collaboration, *ALICE upgrades during the LHC Long Shutdown 2*, 2024 *JINST* **19** P05062 [arXiv:2302.01238] [INSPIRE].

[56] ALICE collaboration, *ALICE technical design report on forward detectors: FMD, T0 and V0*, CERN-LHCC-2004-025 (2004) [INSPIRE].

[57] ALICE collaboration, *Fast Interaction Trigger for ALICE upgrade*, *Nucl. Instrum. Meth. A* **1039** (2022) 167021 [INSPIRE].

JHEP10(2026)057

[58] ALICE collaboration, *Upgrade of the ALICE Readout & Trigger System*, CERN-LHCC-2013-019 (2013) [INSPIRE].

[59] R. Arnaldi et al., *The zero degree calorimeters for the ALICE experiment*, *Nucl. Instrum. Meth. A* **581** (2007) 397 [*Erratum ibid.* **604** (2009) 765] [INSPIRE].

[60] C. Oppedisano et al., *Physics performance of the ALICE zero degree calorimeter*, *Nucl. Phys. B Proc. Suppl.* **197** (2009) 206 [INSPIRE].

[61] I.A. Pshenichnov et al., *Mutual heavy ion dissociation in peripheral collisions at ultrarelativistic energies*, *Phys. Rev. C* **64** (2001) 024903 [nucl-th/0101035] [INSPIRE].

[62] I.A. Pshenichnov, *Electromagnetic excitation and fragmentation of ultrarelativistic nuclei*, *Phys. Part. Nucl.* **42** (2011) 215 [INSPIRE].

[63] ALICE collaboration, *ALICE luminosity determination for Pb–Pb collisions at* $\sqrt{s_{NN}} = 5.02$ *TeV*, 2024 *JINST* **19** P02039 [arXiv:2204.10148] [INSPIRE].

[64] ALICE collaboration, *Neutron emission in ultraperipheral Pb–Pb collisions at* $\sqrt{s_{NN}} = 5.02$ *TeV*, *Phys. Rev. C* **107** (2023) 064902 [arXiv:2209.04250] [INSPIRE].

[65] ALICE collaboration, *Proton emission in ultraperipheral Pb–Pb collisions at* $\sqrt{s_{NN}} = 5.02$ *TeV*, *Phys. Rev. C* **111** (2025) 054906 [arXiv:2411.07058] [INSPIRE].

[66] C. Loizides, J. Nagle and P. Steinberg, *Improved version of the PHOBOS Glauber Monte Carlo*, *SoftwareX* **1-2** (2015) 13 [arXiv:1408.2549] [INSPIRE].

[67] C. Loizides, *Glauber modeling of high-energy nuclear collisions at the subnucleon level*, *Phys. Rev. C* **94** (2016) 024914 [arXiv:1603.07375] [INSPIRE].

[68] C. Loizides, J. Kamin and D. d'Enterria, *Improved Monte Carlo Glauber predictions at present and future nuclear colliders*, *Phys. Rev. C* **97** (2018) 054910 [*Erratum ibid.* **99** (2019) 019901] [arXiv:1710.07098] [INSPIRE].

[69] ALICE collaboration, *Development of the Kalman filter for tracking in the forward muon spectrometer of ALICE*, [ALICE-INT-2003-002].

[70] ALICE collaboration, *Numerical Simulations and Offline Reconstruction of the Muon Spectrometer of ALICE*, [ALICE-INT-2009-044].

[71] P. Buncic, M. Krzewicki and P. Vande Vyvre, *Technical Design Report for the Upgrade of the Online-Offline Computing System*, CERN-LHCC-2015-006 (2015) [INSPIRE].

[72] BES collaboration, $\psi(2S) \to \pi^+\pi^- J/\psi$ *decay distributions*, *Phys. Rev. D* **62** (2000) 032002 [hep-ex/9909038] [INSPIRE].

[73] ALICE collaboration, *First polarisation measurement of coherently photoproduced* J/ψ *in ultra-peripheral Pb–Pb collisions at* $\sqrt{s_{\rm NN}} = 5.02$ *TeV*, *Phys. Lett. B* **865** (2025) 139466 [arXiv:2304.10928] [INSPIRE].

[74] ALICE collaboration, *Quarkonium signal extraction in ALICE*, ALICE-PUBLIC-2015-006 (2015) [INSPIRE].

[75] J.E. Gaiser, *Charmonium Spectroscopy From Radiative Decays of the* J/ψ *and* ψ', SLAC-0255, UMI-83-14449-MC [INSPIRE].

[76] Particle Data Group collaboration, *Review of particle physics*, *Phys. Rev. D* **110** (2024) 030001 [INSPIRE].

[77] H1 collaboration, *Elastic and Proton-Dissociative Photoproduction of* J/ψ *Mesons at HERA*, *Eur. Phys. J. C* **73** (2013) 2466 [arXiv:1304.5162] [INSPIRE].

JHEP10(2026)057

[78] H1 collaboration, *Diffractive photoproduction of $\psi(2S)$ mesons at HERA*, *Phys. Lett. B* **541** (2002) 251 [hep-ex/0205107] [INSPIRE].

[79] ZEUS collaboration, *Measurement of the cross-section ratio $\sigma_{\psi(2S)}/\sigma_{J/\psi(1S)}$ in exclusive photoproduction at HERA*, *JHEP* **12** (2022) 164 [arXiv:2206.13343] [INSPIRE].

[80] G. Baur, K. Hencken and D. Trautmann, *Photon-photon physics in very peripheral collisions of relativistic heavy ions*, *J. Phys. G* **24** (1998) 1657 [hep-ph/9804348] [INSPIRE].

[81] ALICE collaboration, *Measurement of an excess in the yield of J/ψ at very low $p_{\rm T}$ in Pb-Pb collisions at $\sqrt{s_{\rm NN}} = 2.76$ TeV*, *Phys. Rev. Lett.* **116** (2016) 222301 [arXiv:1509.08802] [INSPIRE].

[82] ALICE collaboration, *Photoproduction of low-$p_{\rm T}$ J/ψ from peripheral to central Pb–Pb collisions at 5.02 TeV*, *Phys. Lett. B* **846** (2023) 137467 [arXiv:2204.10684] [INSPIRE].

[83] ALICE collaboration, *Differential studies of inclusive J/ψ and $\psi(2S)$ production at forward rapidity in Pb-Pb collisions at $\sqrt{s_{NN}} = 2.76$ TeV*, *JHEP* **05** (2016) 179 [arXiv:1506.08804] [INSPIRE].

[84] S. Klein and J. Nystrand, *Exclusive vector meson production in relativistic heavy ion collisions*, *Phys. Rev. C* **60** (1999) 014903 [hep-ph/9902259] [INSPIRE].

[85] https://www.hepdata.net/record/ins3155120.

[86] https://github.com/AliceO2Group/O2Physics.

JHEP10(2026)057

The ALICE collaboration

D.A.H. Abdallah[134], I.J. Abualrob[111], S. Acharya[49], K. Agarwal[23,a], G. Aglieri Rinella[32], L. Aglietta[24], N. Agrawal[25], Z. Ahammed[132], S. Ahmad[15], I. Ahuja[36], Z. Akbar[79], V. Akishina[38], M. Al-Turany[93], B. Alessandro[55], A.R. Alfarasyi[100], R. Alfaro Molina[66], B. Ali[15], A. Alici[25,†], J. Alme[20], G. Alocco[24], T. Alt[63], I. Altsybeev[91], C. Andrei[44], N. Andreou[110], A. Andronic[123], M. Angeletti[32], V. Anguelov[90], F. Antinori[53], P. Antonioli[50], N. Apadula[71], H. Appelshäuser[63], S. Arcelli[25,†], R. Arnaldi[55], I.C. Arsene[19], M. Arslandok[135], A. Augustinus[32], R. Averbeck[93], M.D. Azmi[15], B.Kong[69], H. Baba[120], A.R.J. Babu[134], A. Badalà[52], J. Bae[99], Y. Bae[99], Y.W. Baek[99], X. Bai[115], R. Bailhache[63], Y. Bailung[125], R. Bala[87], A. Baldisseri[127], B. Balis[2], S. Bangalia[113], K. Barai[95], V. Barbasova[36], F. Barile[31], L. Barioglio[55], M. Barlou[24], B. Barman[40], G.G. Barnaföldi[45], L.S. Barnby[110], E. Barreau[98], V. Barret[124], L. Barreto[105], K. Barth[32], E. Bartsch[63], N. Bastid[124], G. Batigne[98], D. Battistini[34,91], B. Batyunya[138], L. Baudino[24,b], D. Bauri[46], J.L. Bazo Alba[97], I.G. Bearden[80], D. Behera[47,77], S. Behera[46], M.A.C. Behling[63], I. Belikov[126], V.D. Bella[126], F. Bellini[25], R. Bellwied[111], L.G.E. Beltran[104], Y.A.V. Beltran[43], G. Bencedi[45], O. Benchikhi[73], A. Bensaoula[111], S. Beole[24], A. Berdnikova[90], L. Bergmann[71], L. Bernardinis[23], L. Betev[32], P.P. Bhaduri[132], T. Bhalla[86], A. Bhasin[87], B. Bhattacharjee[40], L. Bianchi[24], J. Bielčík[34], J. Bielčíková[83], A. Bilandzic[91], A. Binoy[113], G. Biro[45], S. Biswas[4], M.B. Blidaru[93], N. Bluhme[38], C. Blume[63], F. Bock[84], T. Bodova[20], L. Boldizsár[45], M. Bombara[36], P.M. Bond[32], G. Bonomi[54,131], H. Borel[127], A. Borissov[138], A.G. Borquez Carcamo[90], E. Botta[24], N. Bouchhar[17], Y.E.M. Bouziani[63], D.C. Brandibur[62], L. Bratrud[63], P. Braun-Munzinger[93], M. Bregant[105], M. Broz[34], G.E. Bruno[31,92], V.D. Buchakchiev[35], M.D. Buckland[82], G.F. Budiski[105], H. Buesching[63], S. Bufalino[29], P. Buhler[73], N. Burmasov[138], Z. Buthelezi[67,119], A. Bylinkin[20], O.B. Bylund[128], J.C. Cabanillas Noris[104], M.F.T. Cabrera[111], H. Caines[135], A. Caliva[28], E. Calvo Villar[97], P. Camerini[23], M.T. Camerlingo[49], S. Cannito[23], S.L. Cantway[135], M. Carabas[108], F. Carnesecchi[32], C. Carr[96], L.A.D. Carvalho[105], J. Castillo Castellanos[127], M. Castoldi[32], F. Catalano[111], S. Cattaruzzi[23], R. Cerri[24], I. Chakaberia[71], P. Chakraborty[133], J.W.O. Chan[111], S. Chandra[132], S. Chapeland[32], M. Chartier[114], S. Chattopadhay[132], M. Chen[39], T. Cheng[6], M.I. Cherciu[62], C. Cheshkov[125], D. Chiappara[27], V. Chibante Barroso[32], D.D. Chinellato[73], F. Chinu[24], J. Cho[57], S. Cho[57], P. Chochula[32], Z.A. Chochulska[133,c], C. Choi[16], P. Choudhary[87], P. Christakoglou[81], P. Christiansen[72], T. Chujo[121], B. Chytla[133], M. Ciacco[24], C. Cicalo[51], G. Cimador[24,32], F. Cindolo[50], F. Colamaria[49], D. Colella[31], A. Colelli[31], M. Colocci[25], M. Concas[32], G. Conesa Balbastre[70], Z. Conesa del Valle[128], G. Contin[23], J.G. Contreras[34], M.L. Coquet[98], P. Cortese[55,130], M.R. Cosentino[107], F. Costa[32], S. Costanza[21], P. Crochet[124], M.M. Czarnynoga[133], A. Dainese[53], E. Dall'occo[32], G. Dange[38], M.C. Danisch[16], A. Danu[62], A. Daribayeva[38], P. Das[32], S. Das[4], A.R. Dash[123], S. Dash[46], A. De Caro[28], G. de Cataldo[49], J. de Cuveland[38], A. De Falco[22], D. De Gruttola[28], N. De Marco[55], C. De Martin[23], S. De Pasquale[28], G.G.A. de Souza[105,d], R. Deb[131], R. Del Grande[34], L. Dello Stritto[32], P. Dhankher[18], D. Di Bari[31], M. Di Costanzo[29], A. Di Mauro[32], B. Di Ruzza[49,129,†], B. Diab[32],

JHEP10(2026)057

K. Dimitrova[35], Y. Ding[6], J. Ditzel[63], R. Divià[32], U. Dmitrieva[55], A. Dobrin[62], B. Dönigus[63], L. Döpper[41], L. Drzensla[2], A. Dubla[93], P. Dupieux[124], T.M. Eder[123], E.C. Ege[63], R.J. Ehlers[71], F. Eisenhut[63], R. Ejima[88,120], D. Elia[49], B. Erazmus[98], F. Ercolessi[25], B. Espagnon[128], G. Eulisse[32], D. Evans[96], F.M.A Smits[112], L. Fabbietti[91], G. Fabbri[50], M. Faggin[32], J. Faivre[70], W. Fan[111], Y. Fan[6], T. Fang[6], A. Fantoni[48], A. Feliciello[55], W. Feng[6], R. Ferioli[34], A. Fernández Téllez[43], B. Fernando[134], L. Ferrandi[105], A. Ferrero[127], C. Ferrero[55,e], A. Ferretti[24], F.M. Fionda[51], A.N. Flores[103], S. Foertsch[67], I. Fokin[90], U. Follo[55,e], R. Forynski[110], E. Fragiacomo[56], H. Fribert[91], J.M. Friedrich[91], U. Fuchs[32], D. Fuligno[23], N. Funicello[28], C. Furget[70], T. Fusayasu[94], J.J. Gaardhøje[80], M. Gagliardi[24], A.M. Gago[97], T. Gahlaut[46], C.D. Galvan[104], S. Gami[77], C. Garabatos[93], J.M. Garcia[43], E. Garcia-Solis[9], S. Garetti[128], C. Gargiulo[32], P. Gasik[93], A. Gautam[113], M.B. Gay Ducati[65], M. Germain[98], R.A. Gernhaeuser[91], M. Giacalone[32], G. Gioachin[29], S.K. Giri[132], P. Giubellino[55], P. Giubilato[27], P. Glässel[90], E. Glimos[118], M.G.F.S.A. Gomes[90], L. Gonella[23], V. Gonzalez[134], M. Gorgon[2], K. Goswami[47], S. Gotovac[33], V. Grabski[66], L.K. Graczykowski[133], E. Grecka[83], A. Grelli[58], C. Grigoras[32], S. Grigoryan[1,138], O.S. Groettvik[32], M. Gronbeck[41], F. Grosa[32], S. Gross-Bölting[93], J.F. Grosse-Oetringhaus[32], R. Grosso[93], N.A. Grunwald[90], R. Guernane[70], M. Guilbaud[98], J.K. Gumprecht[73], T. Gündem[63], T. Gunji[120], J. Guo[10], W. Guo[6], A. Gupta[87], R. Gupta[87], R. Gupta[47], K. Gwizdziel[133], L. Gyulai[45], T. Hachiya[75], C. Hadjidakis[128], F.U. Haider[87], S. Haidlova[34], M. Haldar[4], W. Ham[99], H. Hamagaki[74], R.J. Hamilton[135], Y. Han[137], R. Hannigan[103], J. Hansen[72], J.W. Harris[135], A. Harton[9], M.V. Hartung[63], A. Hasan[117], H. Hassan[112], D. Hatzifotiadou[50], P. Hauer[41], L.B. Havener[135], E. Hellbär[32], H. Helstrup[37], M. Hemmer[63], S.G. Hernandez[111], G. Herrera Corral[8], K.F. Hetland[37], B. Heybeck[63], H. Hillemanns[32], B. Hippolyte[126], I.P.M. Hobus[81], F.W. Hoffmann[38], Y. Hong[57], A. Horzyk[2], Y. Hou[11,93], P. Hristov[32], L.M. Huhta[112], T.J. Humanic[85], V. Humlova[34], M. Husar[122], D. Hutter[38], M.C. Hwang[18], M. Inaba[121], A. Isakov[81], T. Isidori[113], M.S. Islam[46], M. Ivanov[13], M. Ivanov[93], K.E. Iversen[72], M. Jablonski[2], B. Jacak[18,71], N. Jacazio[130], P.M. Jacobs[71], A. Jadlovska[101], S. Jadlovska[101], S. Jaelani[79], J.N. Jager[63], C. Jahnke[106], M.J. Jakubowska[133], E.P. Jamro[2], D.M. Janik[34], M.A. Janik[133], C.A. Jauch[93], S. Ji[16], Y. Ji[93], S. Jia[80], T. Jiang[10], A.A.P. Jimenez[64], S. Jin[10], Z. Jolesz[45], F. Jonas[71], D.M. Jones[114], J.M. Jowett[32,93], J. Jung[63], M. Jung[63], A. Junique[32], J. Juračka[34], J. Kaewjai[100,114], A. Kaiser[32,93], P. Kalinak[59], A. Kalweit[32], H. Kang[12], A. Karasu Uysal[136], N. Karatzenis[96], T. Karavicheva[138], M.J. Karwowska[133], V. Kashyap[77], M. Keil[32], B. Ketzer[41], J. Keul[63], S.S. Khade[47], A. Khatun[129], A. Khuntia[50], Z. Khuranova[63], B. Kileng[37], B. Kim[99], D. Kim[99], D.J. Kim[112], E.J. Kim[68], G. Kim[57], H. Kim[57], J. Kim[137], J. Kim[57], J. Kim[137], J. Kim[32], M. Kim[16], M. Kim[18], S. Kim[17], T. Kim[137], J.T. Kinner[123], I. Kisel[38], A. Kisiel[133], J.L. Klay[5], J. Klein[32], S. Klein[71], C. Klein-Bösing[123], M. Kleiner[63], A. Kluge[32], M.B. Knuesel[135], C. Kobdaj[100], R. Kohara[120], A. Kondratyev[138], J. Konig[63], P.J. Konopka[32], G. Kornakov[133], M. Korwieser[91], C. Koster[81], A. Kotliarov[83], N. Kovacic[122], M. Kowalski[102], V. Kozhuharov[35], G. Kozlov[38], I. Králik[59], A. Kravčáková[36], M.A. Krawczyk[32], L. Krcal[32], F. Krizek[83], K. Krizkova Gajdosova[34],

JHEP10(2026)057

C. Krug[65], M. Krüger[63], E. Kryshen[138], V. Kučera[57], C. Kuhn[126], D. Kumar[132], L. Kumar[86], N. Kumar[86], S. Kumar[49], S. Kundu[32], M. Kuo[121], P. Kurashvili[76], S. Kurita[88], S. Kushpil[83], A. Kuznetsov[138], M.J. Kweon[57], Y. Kwon[137], S.L. La Pointe[38], P. La Rocca[26], A. Lakrathok[100], S. Lambert[98], A.R. Landou[70], R. Langoy[117], P. Larionov[32], E. Laudi[32], L. Lautner[91], R.A.N. Laveaga[104], R. Lavicka[73], R. Lea[54,131], J.B. Lebert[38], H. Lee[99], S. Lee[57], I. Legrand[44], G. Legras[123], A.M. Lejeune[34], T.M. Lelek[2], I. León Monzón[104], M.M. Lesch[91], P. Lévai[45], M. Li[6], P. Li[10], X. Li[10], Z. Liang[115], B.E. Liang-Gilman[18], J. Lien[117], R. Lietava[96], I. Likmeta[111], B. Lim[55], H. Lim[16], S.H. Lim[16], Y.N. Lima[105], S. Lin[10], V. Lindenstruth[38], R. Liotino[31], C. Lippmann[93], D. Liskova[101], D.H. Liu[6], J. Liu[114], Y. Liu[6], G.S.S. Liveraro[106], I.M. Lofnes[20,37], C. Loizides[20], S. Lokos[102], J. Lömker[58], X. Lopez[124], E. López Torres[7], C. Lotteau[125], P. Lu[115], W. Lu[6], Z. Lu[10], O. Lubynets[93], G.A. Lucia[29], F.V. Lugo[66], J. Luo[39], G. Luparello[56], Y.G. Ma[39], R. Mabitsela[119], V. Machacek[80], M. Mager[32], M. Mahlein[91], A. Maire[126], E. Majerz[2], M.V. Makariev[35], G. Malfattore[50], N. Malik[15], N.M. Malik[87], D. Mallick[128], N. Mallick[112], B.M. Mamani[43], G. Mandaglio[30,52], S. Mandal[77], S.K. Mandal[76], A. Manea[62], R. Manhart[91], A.K. Manna[47], F. Manso[124], G. Mantzaridis[91], V. Manzari[49], Y. Mao[6], R.W. Marcjan[2], G.V. Margagliotti[23], A. Margotti[50], A. Marín[93], C. Markert[103], P. Martinengo[32], M.I. Martínez[43], M.P.P. Martins[32,105], S. Masciocchi[93], M. Masera[24], A. Masoni[51], L. Massacrier[128], O. Massen[58], A. Mastroserio[49,129], L. Mattei[24,124], S. Mattiazzo[27], A. Matyja[102], J.L. Mayo[103], F. Mazzaschi[32], M. Mazzilli[31], Y. Melikyan[42], M. Melo[105], A. Menchaca-Rocha[66], J.E.M. Mendez[64], E. Meninno[73], M.W. Menzel[32,90], P.M. Meredith[103], M. Meres[13], R. Michalczyk[133], L. Micheletti[55], D. Mihai[108], D.L. Mihaylov[91], A.U. Mikalsen[20], K. Mikhaylov[138], L. Millot[70], N. Minafra[113,f], D. Miśkowiec[93], A. Modak[56], B. Mohanty[77], M. Mohisin Khan[15,g], M.A. Molander[42], M.M. Mondal[77], S. Monira[133], D.A. Moreira De Godoy[123], A. Morsch[32], C. Moscatelli[23], M.A. Mothibi[67], T. Mrnjavac[32], S. Mrozinski[63], V. Muccifora[48], S. Muhuri[132], A. Mulliri[22], M.G. Munhoz[105], R.H. Munzer[63], L. Musa[32], J. Musinsky[59], J.W. Myrcha[133], B. Naik[119], A.I. Nambrath[18], B.K. Nandi[46], R. Nania[50], E. Nappi[49], A.F. Nassirpour[17], V. Nastase[108], A. Nath[90], N.F. Nathanson[80], A. Neagu[19], L. Nellen[64], R. Nepeivoda[72], S. Nese[19], N. Nicassio[31], B.S. Nielsen[80], E.G. Nielsen[80], Y. Nishida[121], F. Noferini[50], H. Noh[57], S. Noh[12], P. Nomokonov[138], J. Norman[114], N. Novitzky[84], J. Nystrand[20], M.R. Ockleton[114], M. Ogino[74], J. Oh[16], S. Oh[17], A. Ohlson[72], M. Oida[88], L.A.D. Oliveira[106], C. Oppedisano[55], A. Ortiz Velasquez[64], H. Osanai[74], J. Otwinowski[102], M. Oya[88], K. Oyama[74], S. Padhan[131], D. Pagano[54,131], V. Pagliarino[55], G. Paić[64], A. Palasciano[49,92], I. Panasenko[72], P. Panigrahi[46], C. Pantouvakis[27], H. Park[121], J. Park[16], J. Park[68], S. Park[99], T.Y. Park[137], J.E. Parkkila[133], P.B. Pati[80], Y. Patley[46], R.N. Patra[49], J. Patter[47], F. Pazdic[96], H. Pei[6], T. Peitzmann[58], X. Peng[11,53], S. Perciballi[24], G.M. Perez[7], M. Petrovici[44], S. Piano[56], M. Pikna[13], P. Pillot[98], O. Pinazza[32,50], C. Pinto[32], S. Pisano[48], A. Plachta[133], M. Planinic[122], D.K. Plociennik[2], M. Płoskoń[71], S. Politano[32], N. Poljak[122], A. Pop[44], S. Porteboeuf-Houssais[124], J.S. Potgieter[109], E.G. Pottebaum[135], I.Y. Pozos[43], K.K. Pradhan[47], S. Prasad[45,47], S.K. Prasad[4], R. Preghenella[50], F. Prino[55],

JHEP10(2026)057

C.A. Pruneau[134], M. Puccio[32], S. Pucillo[28], S. Pulawski[116], L. Quaglia[24], A.M.K. Radhakrishnan[47], S. Ragoni[14], A. Rakotozafindrabe[127], N. Ramasubramanian[125], L. Ramello[55,130], C.O. Ramírez-Álvarez[43], E. Rao[18], M. Rasa[26], S.S. Räsänen[42], R. Rath[93], M.P. Rauch[20], I. Ravasenga[32], M. Razza[25], K.F. Read[84,118], C. Reckziegel[107], A.R. Redelbach[38], K. Redlich[76,h], H.D. Regules-Medel[43], A. Rehman[20], F. Reidt[32], K. Reygers[90], M. Richter[20], A.A. Riedel[91], W. Riegler[32], A.G. Riffero[24], M. Rignanese[27], C. Ripoli[28], C. Ristea[62], S.B. Rivera[104], M. Rodríguez Cahuantzi[43], K. Røed[19], E. Rogochaya[138], D. Rohr[32], D. Röhrich[20], S. Rojas Torres[34], P.S. Rokita[133], G. Romanenko[25], F. Ronchetti[32], D. Rosales Herrera[43], K. Roslon[133], A. Rossi[53], A. Roy[47], A. Roy[117], S. Roy[46], N. Rubini[50], O. Rubza[15], J.A. Rudolph[81], D. Ruggiano[133], R. Rui[23], P.G. Russek[2], A. Rustamov[78], A. Rybicki[102], L.C.V. Ryder[113], J. Ryu[16], W. Rzesa[91], B. Sabiu[50], R. Sadek[71], S. Sadhu[41], A. Saha[31], S. Saha[46,77], B. Sahoo[47], R. Sahoo[47], D. Sahu[64], P.K. Sahu[60], J. Saini[132], S. Sakai[121], S. Sambyal[87], D. Samitz[73], I. Sanna[32], D. Sarkar[80], V. Sarritzu[22], V.M. Sarti[91], M.H.P. Sas[81], U. Savino[24], S. Sawan[77], E. Scapparone[50], J. Schambach[84], H.S. Scheid[32], C. Schiaua[44], R. Schicker[90], F. Schlepper[32,90], A. Schmah[93], C. Schmidt[93], M. Schmidt[89], J. Schoengarth[63], R. Schotter[73], A. Schröter[38], J. Schukraft[32], K. Schweda[93], G. Scioli[25], E. Scomparin[55], J.E. Seger[14], D. Sekihata[120], M. Selina[81], I. Selyuzhenkov[93], S. Senyukov[126], J.J. Seo[90], L. Serkin[64,i], L. Šerkšnytė[32], A. Sevcenco[62], T.J. Shaba[67], A. Shabetai[98], R. Shahoyan[32], B. Sharma[87], D. Sharma[46], H. Sharma[53], S. Sharma[87], T. Sharma[40], U. Sharma[87], O. Sheibani[134], K. Shigaki[88], M. Shimomura[75], Q. Shou[39], S. Siddhanta[51], T. Siemiarczuk[76], L.L.D. Silva[105], T.F. Silva[105], W.D. Silva[105], D. Silvermyr[72], T. Simantathammakul[100], R. Simeonov[35], B. Singh[46], B. Singh[87], K. Singh[47], R. Singh[77], R. Singh[53], S. Singh[15], T. Sinha[95], B. Sitar[13], M. Sitta[55,130], T.B. Skaali[19], G. Skorodumovs[90], N. Smirnov[135], K.L. Smith[16], R.J.M. Snellings[58], E.H. Solheim[19], S. Solokhin[81], C. Sonnabend[32,93], J.M. Sonneveld[81], F. Soramel[27], A.B. Soto-Hernandez[85], G. Sourpi[32], L.E. Spencer[103], R. Spijkers[81], C. Sporleder[112], I. Sputowska[102], J. Staa[72], J. Stachel[90], L.L. Stahl[105], I. Stan[62], A.G. Stejskal[113], T. Stellhorn[123], S.F. Stiefelmaier[90], D. Stocco[98], I. Storehaug[19], M.M. Storetvedt[37], N.J. Strangmann[63], P. Stratmann[123], S. Strazzi[25], A. Sturniolo[30,52,114], Y. Su[6], A.A.P. Suaide[105], C. Suire[128], A. Suiu[108], M. Suljic[32], V. Sumberia[87], S. Sumowidagdo[79], P. Sun[10], N.B. Sundstrom[58], L.H. Tabares[7], A. Tabikh[70], S.F. Taghavi[91], J. Takahashi[106], M.A. Talamantes Johnson[43], G.J. Tambave[77], Z. Tang[115], J. Tanwar[86], J.D. Tapia Takaki[113], N. Tapus[108], L.A. Tarasovicova[36], M.G. Tarzila[44], A. Tauro[32], A. Tavira García[103,128], G. Tejeda Muñoz[43], L. Terlizzi[24], C. Terrevoli[49], D. Thakur[55], S. Thakur[4], M. Thogersen[19], D. Thomas[103], A.M. Tiekoetter[123], N. Tiltmann[32,123], A.R. Timmins[111], A. Toia[63], R. Tokumoto[88], S. Tomassini[25], K. Tomohiro[88], Q. Tong[6], V.V. Torres[98], A. Trifiró[30,52], T. Triloki[92], A.S. Triolo[32], S. Tripathy[72], T. Tripathy[124], S. Trogolo[24], V. Trubnikov[3], W.H. Trzaska[112], T.P. Trzcinski[133], C. Tsolanta[19], R. Tu[39], R. Turrisi[53], T.S. Tveter[19], K. Ullaland[20], B. Ulukutlu[91], S. Upadhyaya[102], A. Uras[125], M. Urioni[23], G.L. Usai[22], M. Vaid[87], M. Vala[36], N. Valle[54], L.V.R. van Doremalen[58], M. van Leeuwen[81], R.J.G. van Weelden[81], D. Varga[45], Z. Varga[135], P. Vargas Torres[64], O. Vázquez Doce[48], O. Vazquez Rueda[111], G. Vecil[23,b], P. Veen[127], E. Vercellin[24],

JHEP10(2026)057

R. Verma[46], R. Vértesi[45], M. Verweij[58], L. Vickovic[33], Z. Vilakazi[119], A. Villani[23], C.J.D. Villiers[67], T. Virgili[28], M.M.O. Virta[42,80], A. Vodopyanov[138], M.A. Völkl[96], S.A. Voloshin[134], G. Volpe[31], B. von Haller[32], I. Vorobyev[32], J. Vrláková[36], J. Wan[39], C. Wang[39], D. Wang[39], Y. Wang[115], Y. Wang[39], Y. Wang[6], Z. Wang[39], F. Weiglhofer[32], S.C. Wenzel[32], J.P. Wessels[123], P.K. Wiacek[2], J. Wiechula[63], J. Wikne[19], G. Wilk[76], J. Wilkinson[93], G.A. Willems[123], N. Wilson[114], S.L. Winberg[109], B. Windelband[90], J. Witte[90], C.I. Worek[2], J.R. Wright[103], C.-T. Wu[6,27], W. Wu[91], Y. Wu[115], K. Xiong[39], Z. Xiong[115], L. Xu[6,125], R. Xu[6], Z. Xue[71], A. Yadav[41], A.K. Yadav[132], Y. Yamaguchi[88], S. Yang[57], S. Yang[20], S. Yano[88], Z. Ye[71], E.R. Yeats[18], J. Yi[6], R. Yin[39], Z. Yin[6], I.-K. Yoo[16], J.H. Yoon[57], H. Yu[12], S. Yuan[20], A. Yuncu[90], V. Zaccolo[23], C. Zampolli[32], N. Zardoshti[32], P. Závada[61], B. Zhang[90], C. Zhang[127], M. Zhang[6,124], M. Zhang[6,27], S. Zhang[39], X. Zhang[6], Y. Zhang[115], Y. Zhang[115], Z. Zhang[6], M. Zhao[10], D. Zhou[6], Y. Zhou[80], Z. Zhou[39], J. Zhu[39], S. Zhu[93,115], Y. Zhu[6], A. Zingaretti[27], S.C. Zugravel[55], N. Zurlo[54,131]

[1] *A.I. Alikhanyan National Science Laboratory (Yerevan Physics Institute) Foundation, Yerevan, Armenia*
[2] *AGH University of Krakow, Cracow, Poland*
[3] *Bogolyubov Institute for Theoretical Physics, National Academy of Sciences of Ukraine, Kyiv, Ukraine*
[4] *Bose Institute, Department of Physics and Centre for Astroparticle Physics and Space Science (CAPSS), Kolkata, India*
[5] *California Polytechnic State University, San Luis Obispo, California, U.S.A.*
[6] *Central China Normal University, Wuhan, China*
[7] *Centro de Aplicaciones Tecnológicas y Desarrollo Nuclear (CEADEN), Havana, Cuba*
[8] *Centro de Investigación y de Estudios Avanzados (CINVESTAV), Mexico City and Mérida, Mexico*
[9] *Chicago State University, Chicago, Illinois, U.S.A.*
[10] *China Nuclear Data Center, China Institute of Atomic Energy, Beijing, China*
[11] *China University of Geosciences, Wuhan, China*
[12] *Chungbuk National University, Cheongju, Republic of Korea*
[13] *Comenius University Bratislava, Faculty of Mathematics, Physics and Informatics, Bratislava, Slovak Republic*
[14] *Creighton University, Omaha, Nebraska, U.S.A.*
[15] *Department of Physics, Aligarh Muslim University, Aligarh, India*
[16] *Department of Physics, Pusan National University, Pusan, Republic of Korea*
[17] *Department of Physics, Sejong University, Seoul, Republic of Korea*
[18] *Department of Physics, University of California, Berkeley, California, U.S.A.*
[19] *Department of Physics, University of Oslo, Oslo, Norway*
[20] *Department of Physics and Technology, University of Bergen, Bergen, Norway*
[21] *Dipartimento di Fisica, Università di Pavia, Pavia, Italy*
[22] *Dipartimento di Fisica dell'Università and Sezione INFN, Cagliari, Italy*
[23] *Dipartimento di Fisica dell'Università and Sezione INFN, Trieste, Italy*
[24] *Dipartimento di Fisica dell'Università and Sezione INFN, Turin, Italy*
[25] *Dipartimento di Fisica e Astronomia dell'Università and Sezione INFN, Bologna, Italy*
[26] *Dipartimento di Fisica e Astronomia dell'Università and Sezione INFN, Catania, Italy*
[27] *Dipartimento di Fisica e Astronomia dell'Università and Sezione INFN, Padova, Italy*
[28] *Dipartimento di Fisica 'E.R. Caianiello' dell'Università and Gruppo Collegato INFN, Salerno, Italy*
[29] *Dipartimento DISAT del Politecnico and Sezione INFN, Turin, Italy*
[30] *Dipartimento di Scienze MIFT, Università di Messina, Messina, Italy*
[31] *Dipartimento Interateneo di Fisica 'M. Merlin' and Sezione INFN, Bari, Italy*
[32] *European Organization for Nuclear Research (CERN), Geneva, Switzerland*

JHEP10(2026)057

[33] Faculty of Electrical Engineering, Mechanical Engineering and Naval Architecture, University of Split, Split, Croatia
[34] Faculty of Nuclear Sciences and Physical Engineering, Czech Technical University in Prague, Prague, Czech Republic
[35] Faculty of Physics, Sofia University, Sofia, Bulgaria
[36] Faculty of Science, P.J. Šafárik University, Košice, Slovak Republic
[37] Faculty of Technology, Environmental and Social Sciences, Bergen, Norway
[38] Frankfurt Institute for Advanced Studies, Johann Wolfgang Goethe-Universität Frankfurt, Frankfurt, Germany
[39] Fudan University, Shanghai, China
[40] Gauhati University, Department of Physics, Guwahati, India
[41] Helmholtz-Institut für Strahlen- und Kernphysik, Rheinische Friedrich-Wilhelms-Universität Bonn, Bonn, Germany
[42] Helsinki Institute of Physics (HIP), Helsinki, Finland
[43] High Energy Physics Group, Universidad Autónoma de Puebla, Puebla, Mexico
[44] Horia Hulubei National Institute of Physics and Nuclear Engineering, Bucharest, Romania
[45] HUN-REN Wigner Research Centre for Physics, Budapest, Hungary
[46] Indian Institute of Technology Bombay (IIT), Mumbai, India
[47] Indian Institute of Technology Indore, Indore, India
[48] INFN, Laboratori Nazionali di Frascati, Frascati, Italy
[49] INFN, Sezione di Bari, Bari, Italy
[50] INFN, Sezione di Bologna, Bologna, Italy
[51] INFN, Sezione di Cagliari, Cagliari, Italy
[52] INFN, Sezione di Catania, Catania, Italy
[53] INFN, Sezione di Padova, Padova, Italy
[54] INFN, Sezione di Pavia, Pavia, Italy
[55] INFN, Sezione di Torino, Turin, Italy
[56] INFN, Sezione di Trieste, Trieste, Italy
[57] Inha University, Incheon, Republic of Korea
[58] Institute for Gravitational and Subatomic Physics (GRASP), Utrecht University/Nikhef, Utrecht, Netherlands
[59] Institute of Experimental Physics, Slovak Academy of Sciences, Košice, Slovak Republic
[60] Institute of Physics, Homi Bhabha National Institute, Bhubaneswar, India
[61] Institute of Physics of the Czech Academy of Sciences, Prague, Czech Republic
[62] Institute of Space Science (ISS), Bucharest, Romania
[63] Institut für Kernphysik, Johann Wolfgang Goethe-Universität Frankfurt, Frankfurt, Germany
[64] Instituto de Ciencias Nucleares, Universidad Nacional Autónoma de México, Mexico City, Mexico
[65] Instituto de Física, Universidade Federal do Rio Grande do Sul (UFRGS), Porto Alegre, Brazil
[66] Instituto de Física, Universidad Nacional Autónoma de México, Mexico City, Mexico
[67] iThemba LABS, National Research Foundation, Somerset West, South Africa
[68] Jeonbuk National University, Jeonju, Republic of Korea
[69] Korea Institute of Science and Technology Information, Daejeon, Republic of Korea
[70] Laboratoire de Physique Subatomique et de Cosmologie, Université Grenoble-Alpes, CNRS-IN2P3, Grenoble, France
[71] Lawrence Berkeley National Laboratory, Berkeley, California, U.S.A.
[72] Lund University Department of Physics, Division of Particle Physics, Lund, Sweden
[73] Marietta Blau Institute, Vienna, Austria
[74] Nagasaki Institute of Applied Science, Nagasaki, Japan
[75] Nara Women's University (NWU), Nara, Japan
[76] National Centre for Nuclear Research, Warsaw, Poland
[77] National Institute of Science Education and Research, Homi Bhabha National Institute, Jatni, India
[78] National Nuclear Research Center, Baku, Azerbaijan
[79] National Research and Innovation Agency – BRIN, Jakarta, Indonesia

JHEP10(2026)057

[80] Niels Bohr Institute, University of Copenhagen, Copenhagen, Denmark
[81] Nikhef, National institute for subatomic physics, Amsterdam, Netherlands
[82] Nuclear Physics Group, STFC Daresbury Laboratory, Daresbury, U.K.
[83] Nuclear Physics Institute of the Czech Academy of Sciences, Husinec-Řež, Czech Republic
[84] Oak Ridge National Laboratory, Oak Ridge, Tennessee, U.S.A.
[85] Ohio State University, Columbus, Ohio, U.S.A.
[86] Physics Department, Panjab University, Chandigarh, India
[87] Physics Department, University of Jammu, Jammu, India
[88] Physics Program and International Institute for Sustainability with Knotted Chiral Meta Matter (WPI-SKCM^2), Hiroshima University, Hiroshima, Japan
[89] Physikalisches Institut, Eberhard-Karls-Universität Tübingen, Tübingen, Germany
[90] Physikalisches Institut, Ruprecht-Karls-Universität Heidelberg, Heidelberg, Germany
[91] Physik Department, Technische Universität München, Munich, Germany
[92] Politecnico di Bari, Bari, Italy
[93] Research Division and ExtreMe Matter Institute EMMI, GSI Helmholtzzentrum für Schwerionenforschung GmbH, Darmstadt, Germany
[94] Saga University, Saga, Japan
[95] Saha Institute of Nuclear Physics, Homi Bhabha National Institute, Kolkata, India
[96] School of Physics and Astronomy, University of Birmingham, Birmingham, U.K.
[97] Sección Física, Departamento de Ciencias, Pontificia Universidad Católica del Perú, Lima, Peru
[98] SUBATECH, IMT Atlantique, Nantes Université, CNRS-IN2P3, Nantes, France
[99] Sungkyunkwan University, Suwon City, Republic of Korea
[100] Suranaree University of Technology, Nakhon Ratchasima, Thailand
[101] Technical University of Košice, Košice, Slovak Republic
[102] The Henryk Niewodniczanski Institute of Nuclear Physics, Polish Academy of Sciences, Cracow, Poland
[103] The University of Texas at Austin, Austin, Texas, U.S.A.
[104] Universidad Autónoma de Sinaloa, Culiacán, Mexico
[105] Universidade de São Paulo (USP), São Paulo, Brazil
[106] Universidade Estadual de Campinas (UNICAMP), Campinas, Brazil
[107] Universidade Federal do ABC, Santo Andre, Brazil
[108] Universitatea Nationala de Stiinta si Tehnologie Politehnica Bucuresti, Bucharest, Romania
[109] University of Cape Town, Cape Town, South Africa
[110] University of Derby, Derby, U.K.
[111] University of Houston, Houston, Texas, U.S.A.
[112] University of Jyväskylä, Jyväskylä, Finland
[113] University of Kansas, Lawrence, Kansas, U.S.A.
[114] University of Liverpool, Liverpool, U.K.
[115] University of Science and Technology of China, Hefei, China
[116] University of Silesia in Katowice, Katowice, Poland
[117] University of South-Eastern Norway, Kongsberg, Norway
[118] University of Tennessee, Knoxville, Tennessee, U.S.A.
[119] University of the Witwatersrand, Johannesburg, South Africa
[120] University of Tokyo, Tokyo, Japan
[121] University of Tsukuba, Tsukuba, Japan
[122] University of Zagreb Faculty of Science, Department of Physics, Zagreb, Croatia
[123] Universität Münster, Institut für Kernphysik, Münster, Germany
[124] Université Clermont Auvergne, CNRS/IN2P3, LPC, Clermont-Ferrand, France
[125] Université de Lyon, CNRS/IN2P3, Institut de Physique des 2 Infinis de Lyon, Lyon, France
[126] Université de Strasbourg, CNRS, IPHC UMR 7178, F-67000 Strasbourg, France, Strasbourg, France
[127] Université Paris-Saclay, Centre d'Etudes de Saclay (CEA), IRFU, Département de Physique Nucléaire (DPhN), Saclay, France
[128] Université Paris-Saclay, CNRS/IN2P3, IJCLab, Orsay, France
[129] Università degli Studi di Foggia, Foggia, Italy

JHEP10(2026)057

[130] *Università del Piemonte Orientale, Vercelli, Italy*
[131] *Università di Brescia, Brescia, Italy*
[132] *Variable Energy Cyclotron Centre, Homi Bhabha National Institute, Kolkata, India*
[133] *Warsaw University of Technology, Warsaw, Poland*
[134] *Wayne State University, Detroit, Michigan, U.S.A.*
[135] *Yale University, New Haven, Connecticut, U.S.A.*
[136] *Yildiz Technical University, Istanbul, Turkey*
[137] *Yonsei University, Seoul, Republic of Korea*
[138] *Affiliated with an international laboratory covered by a cooperation agreement with CERN*

[a] *Also at INFN Trieste, Trieste, Italy*
[b] *Also at Fondazione Bruno Kessler (FBK), Trento, Italy*
[c] *Also at Czech Technical University in Prague, Prague, Czech Republic*
[d] *Also at Instituto de Fisica da Universidade de Sao Paulo*
[e] *Also at Dipartimento DET del Politecnico di Torino, Turin, Italy*
[f] *Also at University College of Dublin, Dublin, Ireland*
[g] *Also at Department of Applied Physics, Aligarh Muslim University, Aligarh, India*
[h] *Also at Institute of Theoretical Physics, University of Wroclaw, Wroclaw, Poland*
[i] *Also at Facultad de Ciencias, Universidad Nacional Autónoma de México, Mexico City, Mexico*
[†] *Deceased*

JHEP10(2026)057